Uncertainty of the rate parameters of several important elementary reactions of the H_2 and syngas combustion systems

T. Nagy[1,2], É. Valkó[1,3], I. Sedyó[1], I. Gy. Zsély[1], M. J. Pilling[4], T. Turányi[1,*]

[1] Institute of Chemistry, Eötvös University (ELTE), Budapest, Hungary

[2] Institute of Materials and Environmental Chemistry, Research Centre for Natural Sciences of the Hungarian Academy of Sciences, Budapest, Hungary

[3] MTA-ELTE Research Group on Complex Chemical Systems, Budapest, Hungary

[4] School of Chemistry, University of Leeds, Leeds, UK

Abstract

Re-evaluation of the temperature-dependent uncertainty parameter $f(T)$ of elementary reactions is proposed by considering all available direct measurements and theoretical calculations. A procedure is presented for making $f(T)$ consistent with the form of the recommended Arrhenius expression. The corresponding uncertainty domain of the transformed Arrhenius parameters ($\ln A$, n, E/R) is convex and centrally symmetric around the mean parameter set. The $f(T)$ function can be stored efficiently using the covariance matrix of the transformed Arrhenius parameters. The calculation of the uncertainty of a backward rate coefficient from the uncertainty of the forward rate coefficient and thermodynamic data is discussed. For many rate coefficients, a large number of experimental and theoretical determinations are available, and a normal distribution can be assumed for the uncertainty of $\ln k$. If little information is available for the rate coefficient, equal probability of the transformed Arrhenius parameters within their domain of uncertainty (*i.e.* uniform distribution) can be assumed. Algorithms are provided for sampling the transformed Arrhenius parameters with either normal or uniform distributions. A suite of computer codes is presented that allows the straightforward application of these methods. For 22 important elementary reactions of the H_2 and syngas (wet CO) combustion systems, the Arrhenius parameters and 3rd body collision efficiencies were collected from experimental, theoretical and review publications. For each elementary reaction, k_{min} and k_{max} limits were determined at several temperatures within a defined range of temperature. These rate coefficient limits were used to obtain a consistent uncertainty function $f(T)$ and to calculate the covariance matrix of the transformed Arrhenius parameters.

1. **Introduction**

Chemical kinetics databases for many elementary gas-phase reactions provide the recommended values of the Arrhenius parameters, the temperature range of their validity and the uncertainty of rate coefficient k defined by uncertainty parameter f. In combustion chemistry, kinetic data are available from the NIST Chemical Kinetics Database [1], the evaluations of Warnatz [2], Tsang *et al.* (see *e.g.* [3-5]), Baulch *et al.* (see *e.g.*[6-8]) and the review of Konnov [9]. The uncertainty parameter f, which is generally a temperature-dependent value, is defined in the following way:

$$f = \log_{10}\left(k^0/k_{\min}\right) = \log_{10}\left(k_{\max}/k^0\right) \qquad (1)$$

where k^0 is the recommended value of the rate coefficient, $k_{\min}$ and $k_{\max}$ are the extreme, but still not excludable, physically realistic values. This definition of the uncertainty is related to the limits and does not necessarily have a probabilistic inference. According to this approach, the upper and lower extreme values differ from the recommended value by a multiplication factor, which means that, on a logarithmic scale, the extreme values are located symmetrically around the recommended value. In the combustion data collections and evaluations, the uncertainty parameter f is either considered to be temperature independent or it is defined at a few temperatures or in a few temperature intervals.

A detailed probabilistic analysis of the representation of the uncertainty of the rate coefficients in the various databases was recently published in refs. [10] and [11]. A method was provided for determining the covariance matrix of the transformed Arrhenius parameters ($\ln A$, n, E/R) and a continuous uncertainty function $f(T)$ from the uncertainty information given in the databases. This covariance matrix allowed the definition of a multivariate normal distribution and the determination of the uncertainty domain for the transformed Arrhenius parameters [10]. This question is investigated in a wider scope here, considering also the re-evaluation of the uncertainty parameter f, and the case when little information is available for the rate coefficient.

Evaluation of the uncertainty domain of the Arrhenius parameters is very important for the following reasons.

(i) Several chemical kinetics modelling studies use adjusted Arrhenius parameters for a better description of the measured data, and frequently it is not obvious if these modified Arrhenius parameters are physically realistic. Currently it is not easy to check if a newly recommended set of Arrhenius parameters is within its physically realistic domain.

(ii) Frenklach *et al.* (see *e.g.*[12-14]) and Wang *et al.* (see *e.g.*[15-18]) have used systematic optimization of reaction mechanisms to improve the agreement with experimental data. In these studies, selected Arrhenius *A*-factors, 3rd body collision efficiencies and enthalpies of formation were optimized. Fitting may include the optimization of all Arrhenius parameters [19-23]. Application of global optimization methods requires that a physically meaningful uncertainty domain of the parameters (prior uncertainty) is determined first. Then, the optimal parameter set is looked for within this domain. Optimizing all rate parameters of the important reactions may result in a physically more meaningful parameter set than changing the *A*-factors and 3rd body collision efficiencies only. Mechanism optimization results in the posterior stochastic uncertainty of the rate parameters, calculated by methods of mathematical statistics. The posterior uncertainty of the parameters depends on the uncertainty of the experimental data (or theoretical results) used, and the deviation between the data points and the corresponding modelling results based on the optimized reaction mechanism [19].

(iii) Several articles have dealt with the uncertainty analysis of combustion chemistry models [24]. In most of these studies (see *e.g.* [25-33]) only the uncertainty of the Arrhenius parameter *A* was considered, and it was assumed to be equal to the temperature-independent uncertainty of the rate coefficient, characterized by the uncertainty parameter *f*. Maybe the only exception is the recent article of Hébrard *et al.* [34], where the uncertainty of the rate coefficient *k* at 300 K and the uncertainty of the temperature dependence of *k* were considered separately at the uncertainty analysis of an *n*-butane oxidation mechanism. However, Hébrard *et al.* did not consider the joint uncertainty of the Arrhenius parameters. In general, the joint uncertainty of the Arrhenius parameters allows a much more realistic uncertainty analysis of a kinetic model.

The aim of this article is twofold. Firstly, sections 2 to 6 detail the theory of how to obtain the prior uncertainty of the Arrhenius parameters of an elementary reaction based on the information collected from the chemical kinetics literature. Section 2 discusses the determination of the uncertainty domain of the Arrhenius parameters. An uncertainty band of the rate coefficient and the corresponding uncertainty parameter values are obtained in regular temperature intervals (*e.g.* at every 100 K) independently each other from the literature kinetic information. These uncertainty parameter values are denoted as $f_{\text{original}}(T_i)$. In the next step, the uncertainty parameters are made consistent with the form of the Arrhenius expression, yielding uncertainty parameter values $f_{\text{extreme}}(T_i)$. It is shown that the parameters of the extreme Arrhenius curves define a joint uncertainty domain for the transformed Arrhenius parameters, which is centrally symmetric and convex. Section 3 shows that the uncertainty parameter function $f_{\text{extreme}}(T)$ can be efficiently stored in the form of the covariance matrix of the transformed Arrhenius parameters.

The uncertainty parameter function restored from the covariance matrix is denoted $f_{\text{prior}}(T)$. Section 4 presents how the uncertainty of the reverse rate coefficient can be calculated from the uncertainty of the forward rate coefficient and the uncertainty of the thermodynamic data. These methods do not require any assumption for the shape of the probability density function of the Arrhenius parameters. We discuss in Section 5 how to sample efficiently the transformed Arrhenius parameters for parameter optimization or uncertainty analysis applications with either normal or uniform distributions, knowing the covariance matrix and the limits of ln k. Section 6 describes a suite of computer codes related to the procedures above. The Appendix contains the mathematical proofs for the statements of Sections 2 to 6.

The second intention of this article is to review the rate parameters and characterize the uncertainty of 22 elementary reactions important in hydrogen and syngas combustion, to be detailed in Section 7. The rate parameters for these reaction steps, as given in the recent reviews, are listed. A comparison of the parameters of these critical reactions in several recently developed hydrogen and syngas combustion mechanisms is provided. Values of the uncertainty parameter f that are in accordance with the results of all available direct measurements and theoretical calculations for the corresponding reactions are tabulated at several temperatures. The covariance matrix of the transformed Arrhenius parameters was determined from the $T - f$ tables. For the low-pressure limit rate coefficients, 3$^{\text{rd}}$ body collision efficiencies measured in the experiments and used in the various modelling studies are reviewed. An uncertainty range is suggested for each 3$^{\text{rd}}$ body collision efficiency parameter. All collected chemical kinetics information for the investigated elementary reactions are given as Supplementary Material.

2. Uncertainty domain of the Arrhenius parameters

The rate coefficient of an elementary reaction can be determined by experimental methods. If several measurements are carried out in different laboratories (maybe using different methods) at similar temperatures, then the uncertainty of the rate coefficient can be well assessed at a given temperature or in a narrow temperature interval. If the uncertainty of a rate coefficient is determined from literature data independently at different temperatures, then these uncertainties can be very different from each other even at nearby temperatures. However, if the measured rate coefficients are interrelated by a common Arrhenius expression, then the uncertainties measured at different temperatures are also interconnected. Taking into account the temperature dependence of the rate coefficient, the uncertainty at a given temperature cannot be high if it is low at nearby temperatures. This section discusses the determination of an Arrhenius-equation-consistent uncertainty function from the uncertainties of a rate coefficient valid at given temperatures (or in given temperature intervals) and the features of the corresponding uncertainty domain of the Arrhenius parameters.

2.1 The uncertainty band of Arrhenius curves

The temperature dependence of rate coefficient k is described by the modified Arrhenius equation $k=A\ \{T\}^n \exp(-E/RT)$. In accordance with the recommendations [35], curly brackets are used to denote the numerical value of the enclosed physical quantity at the predefined units, which are cm, K, s, mol in this paper. Introducing transformed parameters $\kappa(T) := \ln\{k(T)\}$, $\alpha := \ln\{A\}$ and $\varepsilon := E/R$, the linearized form of the modified Arrhenius equation is

$$\kappa(T) = \alpha + n \ln\{T\} - \varepsilon\, T^{-1} \qquad (2)$$

In the chemical kinetics literature both the original parameters (A, n, E) and the transformed parameters ($\ln\{A\}$, n, E/R) are referred to as Arrhenius parameters. In this article, term Arrhenius parameters is always used for the transformed ones.

The procedure described here determines the uncertainty domain of Arrhenius parameters ($\mathbf{p}=(\alpha,n,\varepsilon)^{\mathrm{T}}$) from the uncertainty information for the rate coefficients. In several cases the temperature dependence of the rate coefficient can be described by two Arrhenius parameters (α,ε) or (α,n). In this case the third Arrhenius parameter is set to zero.

Assume that a central set of Arrhenius parameters $\mathbf{p}^0$ is available and the symmetric uncertainty of the rate coefficient is estimated at several temperatures by uncertainty parameters $f(T_i)$, i = 1, … , n_T. It is possible to generate all Arrhenius curves $\kappa(T,\mathbf{p})$ that lie between the uncertainty limits, fulfilling the following $2n_T$ inequalities.

$$-f(T_i) \le \frac{\kappa(T_i;\mathbf{p}) - \kappa(T_i;\mathbf{p}^0)}{\ln 10} \le +f(T_i) \qquad i = 1,\ldots,n_T \tag{3}$$

These curves are located symmetrically around the mean rate coefficient curve $\kappa(T;\mathbf{p}^0)$, since Arrhenius equation (2) is a linear function of parameters α, n, ε and equation (3) defines symmetric linear constraints. A systematic procedure is proposed here for determining the extreme Arrhenius curves, which touch either the lower or the upper uncertainty limit at least at 2 or 3 temperatures for the 2- and the 3-parameter cases, respectively, and also go within the upper and lower uncertainty limits at all other temperatures. Formally, these criteria correspond to Arrhenius functions that fulfil at least 2 or 3 equality relations in equations (3) and for the remaining $2n_T$–2 or $2n_T$–3 cases, respectively, either the equality or the inequality is fulfilled. The minimum and maximum values of these curves at a given temperature define the edges of the band of all possible Arrhenius curves.

In the case of the 3-parameter Arrhenius expression, term $n\cdot\ln\{T\}$ usually has a smaller contribution to the temperature dependence of the rate coefficient than $-\varepsilon/T$, since $\ln\{T\}$ changes more slowly than $1/T$ at combustion temperatures. The effect of a change in the temperature exponent n on the rate coefficient at high temperatures can be well compensated by adjusting the pre-exponential factor α, leading to a very strong anti-correlation between α and n in most determinations. This implies that values of n, which significantly deviate (*i.e.* by ±10) from the central n^0, can also fulfil all the inequality requirements in equation (3) if the initial uncertainty limits are not too tight. Both theoretical considerations [36] and the typical range of values of n in kinetic databases [1] show that the temperature exponent n of elementary chemical reactions should take values of small negative and positive numbers. Therefore, we recommend confining the range of n values to a narrow (*i.e.* Δn = 2) symmetric interval around the central value n^0 when the band of possible Arrhenius curves is determined through finding extreme Arrhenius curves.

$$-\Delta n \le n - n^0 \le +\Delta n \tag{4}$$

The extreme Arrhenius curves are those which fulfil at least 2 or 3 equality relations in equations (3) and (4) for the two-parameter and the three-parameter cases, respectively. To determine the extreme Arrhenius curves, uncertainty values need to be known at least at 2 temperatures, since in the three-parameter case a constraint is given for parameter n.

The procedure is demonstrated on the reaction $H_2O_2+H \rightarrow H_2O+OH$ of the (α,ε)-type and the reaction $H+CH_3 \rightarrow H_2+{}^1CH_2$ of the (α,n,ε)-type; the recommended Arrhenius parameters and uncertainty f values are shown in Table 1. The first reaction is evaluated in this work as reaction R14 (see Section 7.3), while the data for the second reaction were taken from Baulch *et al.* [8]. Fig. 1 shows the values of the original uncertainty limits and the continuous curve of the new uncertainty limits. The original uncertainty limits are shown at every 100 K within the temperature range of validity [T_{min},T_{max}], leading to $2n_T$ uncertainty limits (see equation 3), where n_T=[(T_{max}–T_{min})/100 K]+1. Due to this discretization a finite number of extreme Arrhenius curves can be determined depending on the number of points considered. However, some of these curves may coincide.

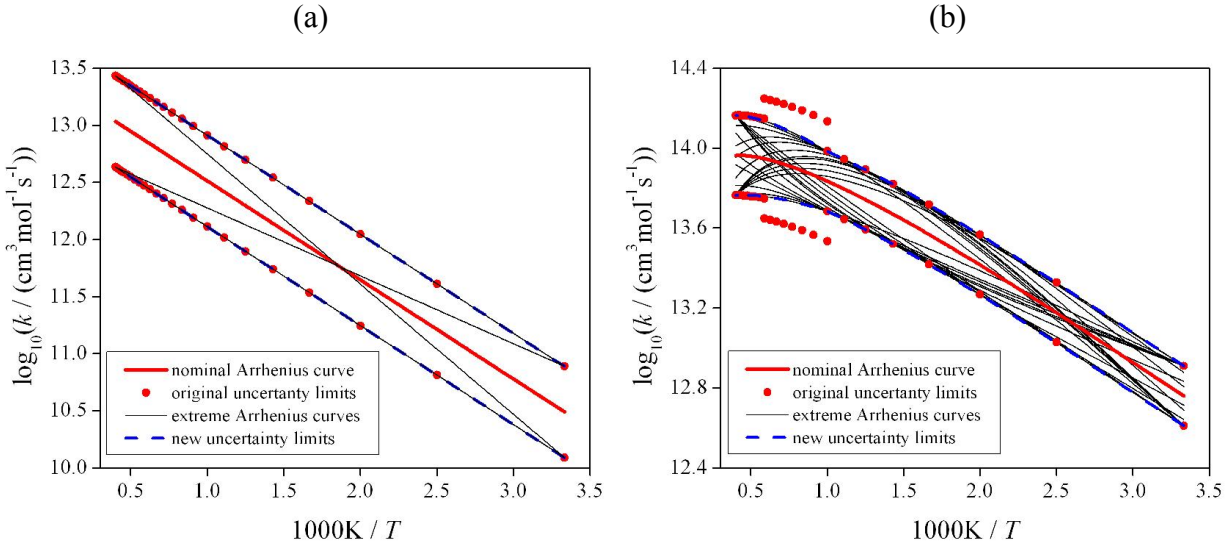

Fig. 1. The uncertainty band of Arrhenius curves is determined by drawing all extreme Arrhenius curves (black thin solid lines) going between the original uncertainty limits (red dots), which are symmetrically located around the mean curve (red thick solid line), and determining the extrema of this series of curves (blue dashed lines). Figures 1a and 1b correspond to reactions $H_2O_2+H \rightarrow H_2O+OH$ and $H+CH_3 \rightarrow H_2+{}^1CH_2$.

For the (α,ε)-type example reaction H_2O_2+H→H_2O+OH with constant uncertainty, only four distinct extreme Arrhenius curves (straight lines in an Arrhenius plot) can be found and the corresponding new uncertainty limits coincide with the original uncertainty limits (see Fig. 1a). For the (α,n,ε)-type example reaction H+CH_3→H_2+$^1CH_2$ with piece-wise constant uncertainty, several different extreme Arrhenius curves can be defined using the discretized uncertainty curve (see Fig. 1b). Although we assumed Δn=2 for the maximal allowed deviation of temperature exponent n, the $|n-n^0|$ value of the extreme Arrhenius curves was always less than 2 in this case.

2.2 Uncertainty parameter function f(T) consistent with the Arrhenius equation

The minimum and maximum values of the extreme Arrhenius curves ($\kappa_{min}(T)$ and $\kappa_{max}(T)$) define new uncertainty limits, which are symmetrically located around the mean $\kappa(T;\mathbf{p}^0)$ curve. These new limits, obtained from a set of uncertainty values f and a user-defined Δn, uniquely define a new, continuous uncertainty function $f_{extreme}(T)$:

$$f_{extreme}(T) = \frac{\kappa\left(T;\mathbf{p}^0\right) - \kappa_{min}\left(T\right)}{\ln 10} \equiv \frac{\kappa_{max}\left(T\right) - \kappa\left(T;\mathbf{p}^0\right)}{\ln 10} \tag{5}$$

By definition, this Arrhenius-equation-consistent uncertainty $f_{extreme}(T_i)$ is always less than or equal to the original uncertainty $f(T_i)$ at every temperature T_i (i=1,..,n_T). Fig. 2 shows the values of original uncertainty parameters and the curves of the new uncertainty functions for reactions H_2O_2+H→H_2O+OH (Fig. 2a) and H+CH_3→H_2+$^1CH_2$ (Fig. 2b), *i.e.* for the same reactions that were used in Fig. 1.

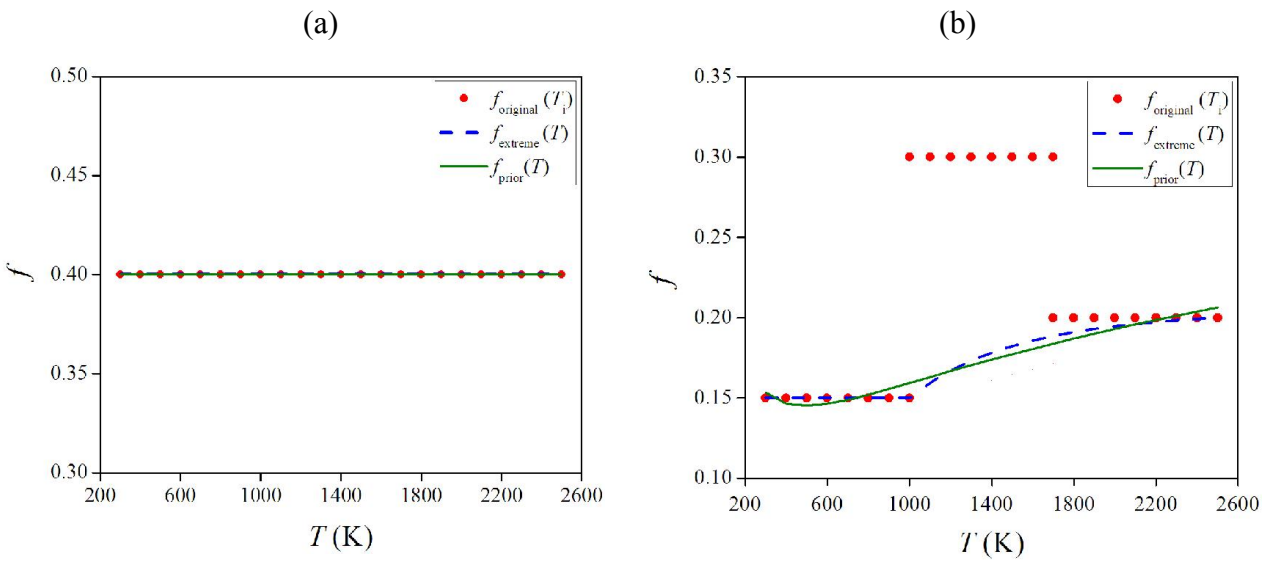

Fig. 2. Temperature dependence of uncertainty parameter f for reactions $H_2O_2+H \rightarrow H_2O+OH$ (a) and $H+CH_3 \rightarrow H_2+{}^1CH_2$ (b). The original uncertainty parameters ($f_{original}$, red dots) are taken from evaluations of kinetic data (this work and Baulch *et al.* [8], respectively). The Arrhenius-equation-consistent uncertainty parameters ($f_{extreme}$, blue dashed line) are determined from the band of all allowed Arrhenius curves going between the original limits (see Fig. 1). Uncertainty parameters f_{prior} (green solid line) are calculated from the fitted covariance matrix of the Arrhenius parameters**.**

Since κ is a linear function of the Arrhenius parameters (see Eq. (2)), the new uncertainty function $f_{extreme}$ depends only on the original f values and on the value of Δn, but it is independent from the mean values of the Arrhenius parameters. For the two-parameter example (Fig 2a) the original, constant uncertainty parameter was consistent with the Arrhenius form ($f_{original}=f_{extreme}$). For reaction $H+CH_3 \rightarrow H_2+{}^1CH_2$ (Fig 2b), at intermediate temperatures there are few reliable measurements, therefore higher uncertainty was assigned in the middle temperature region. This is correct, if the experimental uncertainties are handled independently in the various temperature regions. Taking into account that the prior uncertainty should be consistent with the Arrhenius expression in the whole temperature region, a significantly lower $f_{extreme}$ uncertainty was obtained at intermediate temperatures (1000–1700 K). In this case, uncertainty information $f_{original}$ can be considered as redundant at temperatures where $f_{original}>f_{extreme}$, therefore f(300–1000 K)=0.15 and f(2500 K)=0.2 represent the same information as the original evaluated uncertainty. In the general case, of course, not necessarily the uncertainties at the middle temperatures are inconsistent with the other ones. The presented procedure is able to correct all high uncertainties that are not consistent with lower uncertainties, determined at other temperatures.

2.3 Properties of the uncertainty domain of the Arrhenius parameters

Parameters (α,n,ε) of the possible Arrhenius curves, which fulfil inequalities in equations (3) and (4), form the uncertainty domain of Arrhenius parameters. According to the mathematical proof presented in Appendix 1, any convex linear combination of the parameter sets of extreme Arrhenius curves provides a possible Arrhenius set. This implies that the domain of possible Arrhenius parameters is convex and the vertices of the convex shell are given by the parameters of the extreme Arrhenius curves. This means that if two or more sets of Arrhenius parameters are within this domain, then any convex linear combination of them is also within the domain. It is also proved in Appendix 1 that the uncertainty domain of the Arrhenius parameters is centrally symmetric for mirroring through the point of central Arrhenius parameters $\mathbf{p}^0$. Furthermore, the symmetric domain around $\mathbf{p}^0$ will define a symmetric uncertainty range in κ at every temperature, allowing the unique definition of the uncertainty function $f_{\text{extreme}}(T)$.

As discussed in Section 2.1, for the (α,ε)-type example reaction with constant uncertainty (reaction $H_2O_2+H \rightarrow H_2O+OH$), there are only four possible extreme curves, which are drawn as thin black lines in Fig. 1a. Parameters of these extreme Arrhenius curves correspond to four corners of a parallelogram on the (α,ε) plane (see Fig. 3a) and all possible Arrhenius parameters are within this parallelogram, which is a convex shape.

A three-parameter (α,n,ε) Arrhenius expression with constant uncertainty parameter f defines a convex 3D uncertainty domain of curved irregular shape, which has an infinite number of vertices, corresponding to the infinite number of extreme Arrhenius curves. For the second example (reaction $H+CH_3 \rightarrow H_2+{}^1CH_2$), the uncertainty function f_{extreme} is constant below 1000 K and temperature dependent above 1000 K (see Fig. 2b), thereby the corresponding uncertainty domain of Arrhenius parameters has a non-regular shape (see Fig. 3b). Its surface is a convex polyhedron and not curved, because uncertainty function f_{extreme} was approximated by a finite number of points.

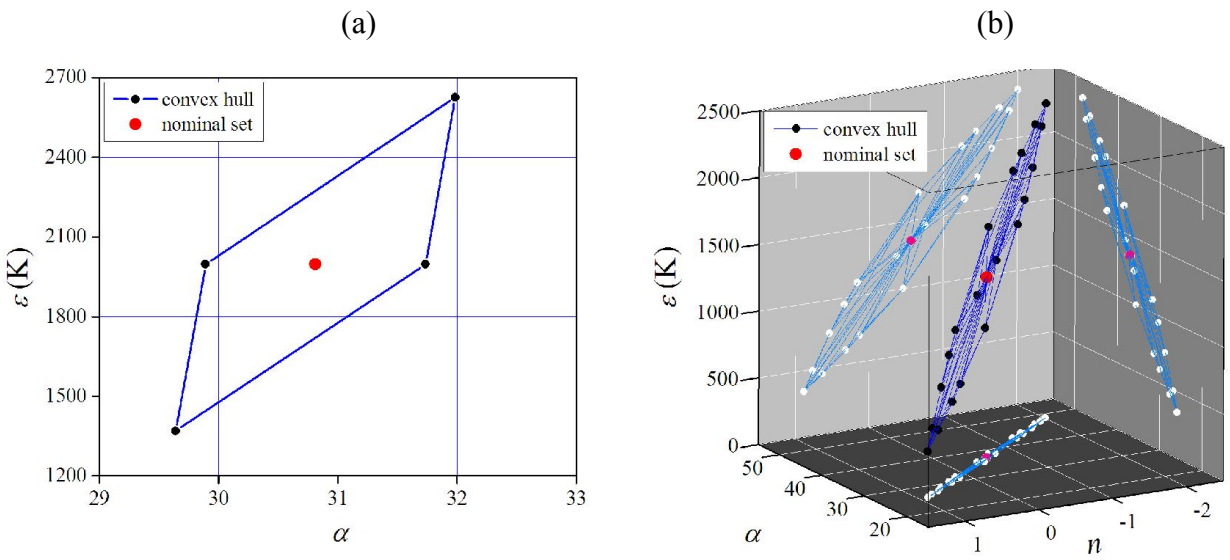

Fig. 3. Convexity and symmetry of the uncertainty domain of Arrhenius parameters is shown for the two examples that have been used in Figs. 1 and 2. In both figures a) and b), the large red dot represents the mean set $\mathbf{p}^0$ of the Arrhenius parameters. The small black dots correspond to the Arrhenius parameters of the extreme Arrhenius curves (see Fig. 1) and span the vertices (dark blue lines) of the convex hull. In the 3-parameter case, the sides of the convex hull are defined by the triangles between these vertices. In Fig. 3b, the projections of the mean value and the convex hull to the α–n, α–ε, and n–ε planes are indicated with white dots and light blue lines.

3. Efficient storage of the uncertainty domain

In the previous section the determination of a consistent uncertainty band of the rate coefficient is described and the features of the corresponding joint uncertainty domain of the Arrhenius parameters are discussed. This uncertainty domain may have a very different shape depending on the temperature dependence of the original uncertainty parameters. In this section we show that the shape of uncertainty band of the rate coefficients, and therefore also the uncertainty domain of the Arrhenius parameters can be represented with a few numbers only. These are the 6 parameters of the covariance matrix of the extended Arrhenius expression. If the temperature dependence is described by a 2-parameter Arrhenius expression ((α,ε) or (α,n) types), the uncertainty can be defined by the 3 parameters of the covariance matrix. The determination of the covariance matrix of the Arrhenius parameters has been discussed in our previous publications [10] [11], in the context of the probabilistic interpretation of the uncertainty information in the databases.

The temperature-dependent rate coefficient $k(T)$ (and its natural logarithm $\kappa(T)$) can be considered as a random variable deduced from measurements and calculations. Assuming a probabilistic meaning to f_{extreme}, that is if f_{extreme} corresponds to 3 standard deviations (3σ) [25-30])) or 2 standard deviations (2σ) [16-18] of the untruncated distribution of rate coefficient on a decimal logarithmic scale, the uncertainty parameter f can be converted [26] to the standard deviation of the natural logarithm of the rate coefficient (σ_κ) at a given temperature T:

$$\sigma_\kappa(T) = \frac{\ln 10}{\mu} f(T) \tag{6}$$

where parameter μ is usually assumed to be 3 or 2, respectively.

Arrhenius parameters α, n, and ε are also random values, since these can be calculated from the random values of $\kappa(T)$ at three given temperatures using the linearized Arrhenius equation (see Eq. (2)). The joint probability density function of the Arrhenius parameters is independent of temperature. This means that all central moments are also independent of temperature, including their expected values ($\overline{\alpha}$, $\overline{n}$, $\overline{\varepsilon}$), variances ($\sigma_\alpha^2, \sigma_n^2, \sigma_\varepsilon^2$) and correlations ($r_{\alpha n}$, $r_{\alpha\varepsilon}$, $r_{\varepsilon n}$).

The following relation was deduced [10] between the variance of $\kappa(T)$ and the elements of the covariance matrix of the Arrhenius parameters:

$$\begin{aligned}\sigma_\kappa^2(T) &= \boldsymbol{\Theta}^{\mathrm{T}} \boldsymbol{\Sigma}_{\mathbf{p}} \boldsymbol{\Theta} = \\ &= \sigma_\alpha^2 + \sigma_n^2 \ln^2 T + \sigma_\varepsilon^2 T^{-2} + 2 r_{\alpha n} \sigma_\alpha \sigma_n \ln T - 2 r_{\alpha\varepsilon} \sigma_\alpha \sigma_\varepsilon T^{-1} - 2 r_{n\varepsilon} \sigma_n \sigma_\varepsilon T^{-1} \ln T\end{aligned} \tag{7}$$

A method was proposed [10] for the determination of the covariance matrix of the Arrhenius parameters using equations (6) and (7) from uncertainty parameter f of the rate coefficient at various temperatures. To determine the elements of the covariance matrix for the three-parameter Arrhenius expression, the uncertainty of the rate coefficient has to be known at least at six different temperatures. In the (α,ε) and (α,n) two-parameter cases, the uncertainty of the corresponding Arrhenius parameters can be handled in a similar way and the uncertainty of the rate coefficient has to be known at least at three temperatures [10].

Disregarding the possible stochastic meaning of uncertainty f, the equations (6) and (7) provide a means for storing the $f_{\text{extreme}}(T)$ function in the form of the covariance matrix of Arrhenius parameters. The uncertainty function reconstructed from the covariance matrix is called here prior uncertainty and denoted as $f_{\text{prior}}(T)$. Despite there being no formal mathematical relationship between f_{extreme} and f_{prior}, function $f_{\text{extreme}}(T)$ could always be well approximated by $f_{\text{prior}}(T)$ in all of our investigated cases of more than 30 elementary reactions. Figure 2 shows the determined $f_{\text{prior}}(T)$ functions for the two example reactions. For the constant uncertainty case, it

coincides with the $f_{\mathrm{extreme}}(T)$ curve, whereas for the three-parameter example it approximates well the corresponding $f_{\mathrm{extreme}}(T)$ function.

In equation (6), the parameter μ defines the proportionality between the uncertainty parameter f and the standard deviation σ_κ. When the uncertainty f_{prior} is calculated via σ_κ from the covariance matrix $\mathbf{\Sigma_p}$, the same parameter μ has to be used. This means that the value of μ is arbitrary in the storage of the f values in the covariance matrix, and the only important assumption here is that the uncertainty parameter f is proportional to the standard deviation of κ.

4. Uncertainty of the Arrhenius parameters of the reverse reaction

In the case of many elementary reactions, the rate coefficients can be measured for both the forward and reverse directions. Frequently, for technical reasons, the rate coefficient is determined in one direction at low temperatures and in the opposite direction at high temperatures. The thermodynamic equilibrium constant relates the rate coefficients for the two opposing directions, and the uncertainties of the rate coefficients for the two directions can also be related by considering the uncertainty of the equilibrium constant. This latter relationship is significant because the assessed uncertainty of the rate coefficient is better established if data for both directions are taken into account.

If the Arrhenius parameters of the forward reaction are known, rate coefficient k_f can be calculated at any temperature T, knowing the standard reaction enthalpy $\Delta_r H^{\ominus}$ and standard reaction entropy $\Delta_r S^{\ominus}$. The calculation is discussed in several textbooks (see *e.g.* [37]) and uses the following sequence of equations: $\Delta_r G^{\ominus} = \Delta_r H^{\ominus} - T\,\Delta_r S^{\ominus}$, $\Delta_r G^{\ominus} = -RT \ln K$, $K_c = K \left(p^{\ominus}/RT\right)^{\sum_i \nu_i}$, and $k_b = k_f / K_c$ where K and K_c are the equilibrium constants expressed in normalized pressures and molar concentrations, respectively, and coefficients ν_i are the stoichiometric coefficients.

Combining all these equations and taking the natural logarithm of both sides gives the following equation:

$$\ln\{k_{\mathrm{b}}\} = \ln\{k_{\mathrm{f}}\} + \frac{\Delta_r H^{\ominus}}{RT} - \frac{\Delta_r S^{\ominus}}{R} - \sum \nu_{\mathrm{i}} \cdot \ln\left\{\frac{p^{\ominus}}{RT}\right\} \qquad (8)$$

Note that common physical base units have to be used within the curly brackets.

At a given temperature T, the last term on the right hand side of equation (8) is constant, thus this term has no uncertainty. The standard reaction entropy for small species can be calculated

with high accuracy [28]; therefore, the uncertainty of the corresponding term is also negligible. This is not true for larger non-rigid molecules and radicals, where the calculated conformational entropy may have significant uncertainty at higher temperatures. Both forward rate coefficient k_f and standard reaction enthalpy $\Delta_r H^{\ominus}$ have relatively high uncertainty and these can be considered to be uncorrelated. If the uncertainty of the entropy term can be neglected, then the variance of rate coefficient k_b can be calculated in the following way:

$$\sigma^2(\ln\{k_b\}) = \sigma^2(\ln\{k_f\}) + \frac{\sigma^2(\Delta_r H^{\ominus})}{(RT)^2} \tag{9}$$

This equation implies that if the uncertainty of the standard reaction enthalpy is small compared to the uncertainty of k_f, then the uncertainty f belonging to the rate coefficients of the forward and backward reactions can be considered to be equal.

The reaction enthalpy can be calculated as the linear combination of the standard enthalpies of formation of the participating species:

$$\Delta_r H^{\ominus} = \boldsymbol{\nu}^T \Delta \mathbf{H}_f^{\ominus} = \Delta \mathbf{H}_f^{\ominus T} \boldsymbol{\nu} \tag{10}$$

Here, $\boldsymbol{\nu}$ and $\Delta \mathbf{H}_f^{\ominus}$ are the column vectors of stoichiometric coefficients and the standard enthalpies of formation, respectively. The variance of the reaction enthalpy can be calculated from the covariance matrix of the standard enthalpies of formation of the participating species.

$$\begin{aligned} \sigma^2\left(\Delta_r H^{\ominus}\right) &= \overline{(\Delta_r \mathbf{H}^{\ominus} - \overline{\Delta_r \mathbf{H}^{\ominus}})(\Delta_r \mathbf{H}^{\ominus} - \overline{\Delta_r \mathbf{H}^{\ominus}})^T} = \\ &= \boldsymbol{\nu}^T \overline{(\Delta \mathbf{H}_f^{\ominus} - \overline{\Delta \mathbf{H}_f^{\ominus}})(\Delta \mathbf{H}_f^{\ominus} - \overline{\Delta \mathbf{H}_f^{\ominus}})^T} \boldsymbol{\nu} = \boldsymbol{\nu}^T \boldsymbol{\Sigma}_{\Delta H_f^{\ominus}} \boldsymbol{\nu} \end{aligned} \tag{11}$$

where $\boldsymbol{\Sigma}_{\Delta H_f^{\ominus}}$ is the covariance matrix of the standard enthalpies of formation.

The traditional thermodynamic databases contain the enthalpies of formation of the species and their standard deviation at 298 K. The Active Thermochemical Tables (ATcT) approach [38, 39] and the NEAT method [40] also provide information about the correlation of the enthalpies of formation. Using Kirchoff's law, the uncertainty of the standard reaction enthalpy at higher temperatures are related to the uncertainties in heat capacities of species, which can also be considered to be small. Consequently, the uncertainty in the reaction enthalpy at 298 K may also be used as an approximation at higher temperatures.

5. Assuming a given distribution of the Arrhenius parameters

Until this point, no particular form of the distribution of the Arrhenius parameters within the uncertainty domain was assumed. At the beginning of Section 3, it was assumed that uncertainty parameter f is proportional to the standard deviation of κ with proportionality constant (ln 10)/μ. However, the chemical kinetics databases define parameter f as extreme deviations from $\log_{10}\{k^0\}$, therefore the distribution has to be truncated at these limits. If the original (not truncated) probability density function of κ has the feature that the points outside of the truncation limits have small probability, then the covariance matrix statistically well characterizes also the truncated distribution of Arrhenius parameters. This is the case for a normal distribution with μ= 3 or 2, when the probabilities of κ values outside the 3σ (or 2σ) limits are only 0.0027 and 0.0455, respectively. In the case of a normal distribution it can be consistently assumed that κ at every temperature and the Arrhenius parameters (α,n,ε) have single and multivariate normal distributions, respectively [10]. Furthermore, the standard deviations of κ and the covariance matrices of Arrhenius parameters for the truncated and untruncated normal distributions are approximately the same. On the contrary, in the case of a uniform distribution of Arrhenius parameters the covariance matrix $\mathbf{\Sigma_p}$, used for storing the uncertainty function, does not characterize statistically the distribution of the Arrhenius parameters. In addition, the distribution of κ values at various temperatures will neither be uniform nor will have the same shape at all temperatures, therefore the ratio of the truncation limits and the standard deviation of κ will be temperature dependent.

Here we discuss in detail the cases of normal and uniform probability distributions. It will be shown that in both cases the probability distribution of the Arrhenius parameters can be reconstructed from the covariance matrix $\mathbf{\Sigma_p}$, which is used for storing $f_{\text{prior}}(T)$. We note that the probability distribution of the parameters is required by several global uncertainty analysis methods [24]. Taking into account not only the domain of uncertainty, but also the probabilistic information on the Arrhenius parameters makes the uncertainty calculations more realistic. Also, several mechanism optimization and parameter estimation methods require a realistic prior distribution of the varied parameters. It makes the procedure more effective, since the search for the optimal parameters can be started from the region of Arrhenius parameters that has higher probability according to the literature information.

5.1 Normal distribution

For the rate coefficients of several hundred elementary gas-phase reactions, dozens of measurements and theoretical calculations are available. Their results are usually centred on the evaluated rate coefficients, while fewer determinations support values close to the uncertainty limits. Consequently, the Arrhenius parameters recommended in the data evaluations have high probability, while the values at the edge of the uncertainty domain of the Arrhenius parameters have low probability. According to the central limit theorem, if a variable is obtained as a sum of several independent random variables, then the distribution of this variable is of nearly normal distribution.

It has been proven in our previous article that if the Arrhenius parameters have multivariate normal distribution, then the calculated κ will have a normal distribution at any temperature [10]. Also, if κ follows a normal distribution at many temperatures, then the most natural, consistent assumption is that (α,n,ε) follow a multivariate normal distribution [10]. The knowledge of the mean values and the covariance matrix of the Arrhenius parameters allows the definition of a multivariate normal distribution, which can be sampled according the procedure discussed in the appendix of our previous work [10]. In this work, $\mu = 3$ and hence the normal distribution of κ truncated at 3σ deviations is assumed in equation (6).

The assumption of a normal distribution is also applicable for the case of backward reactions. It is frequently assumed that the enthalpies of formation and the $\ln\{k_f\}$ values have normal distributions. Any linear function of normally distributed independent random variables also follows a normal distribution; therefore $\ln\{k_b\}$ will also be normally distributed in equation (8).

5.2 Uniform distribution

Frequently only a few measurements exist for an investigated reaction, and therefore a temperature-independent uncertainty parameter f is recommended or uncertainty parameter values are suggested at few temperatures only. In this case, considering equal probability (*i.e.* uniform distribution) for any possible set of Arrhenius parameters (α,n,ε) is the appropriate *a priori* assumption during the optimization or uncertainty analysis of a kinetic model. Assuming a uniform distribution as a prior distribution in parameter optimization has the advantage that none

of the parameter sets is privileged. The disadvantage of a uniform distribution is that the assumed probability at the uncertainty limits is equal to that of the mean value, and it drops to zero just outside the limits. This section presents an algorithm for the generation of sets of Arrhenius parameters with uniform distributions within their domain of uncertainty. The algorithm describes the (α,n,ε) three-parameters case, and a similar algorithm is applicable for the (α,ε) and (α,n) two-parameters cases.

The covariance matrix is able to store efficiently the $f_{\text{extreme}}(T)$ function, but it does not characterize statistically the uniform distribution of **p**. However, the domain of the uniform distribution of the Arrhenius parameters can be reconstructed from the $f_{\text{prior}}(T)$ function parameterized by the covariance matrix. When a uniform distribution is assumed, the selection of μ is arbitrary; we used $\mu = 3$ in equation (6) in our studies.

The first step is sampling $\kappa(T_i)$ values at three different selected temperatures T_i from a uniform distribution within their range of uncertainty determined by $f_{\text{prior}}(T_i)$. It is shown in Appendix 2 that if the $\kappa(T_i)$ values have uniform distributions, then the Arrhenius parameters obtained by solving equation (2) at three temperatures also have uniform distributions. The **p** parameters obtained are checked and those values are discarded that have the parameter value n outside the predefined limits or correspond to Arrhenius curves going outside the uncertainty limits of κ at any other temperature (see equations (3) and (4)). It is shown in Appendix 1 that the distribution of Arrhenius parameters obtained after discarding these sets will also be uniform, and its domain remains convex and symmetric. By this means, the uncertainty domain of the Arrhenius parameters can be evenly sampled in an efficient way.

The domain and distribution obtained do not depend on the initial selection of the three temperatures where the $\kappa(T_i)$ values are sampled, but a good selection may improve the effectiveness of the sampling procedure. The recommended selection of sampling points are the two edges of the temperature interval and/or the temperatures with the lowest uncertainty, since this choice usually leads to low number of rejected Arrhenius curves, which go outside the allowed ranges of κ at least at one of the other temperatures or that of n.

We emphasize that this section discussed the case of the uniform distribution of the Arrhenius parameters, which does not imply that the distribution of κ is uniform at all temperatures. As equation (2) shows, κ is a weighted sum of three random variables with joint uniform distribution over a convex and symmetric domain, which results in a higher probability near the mean κ^0 value.

6. Software tools

For the determination of the uncertainty limits of the rate coefficients, the joint uncertainty domain and the probability distribution of rate parameters, and for their efficient sampling, four computer codes called *u-Limits*, UBAC, JPDAP and SAMAP were developed and used in this work. These computer codes, together with their user manual, can be freely downloaded from our Web site [41]. JPDAP has already been made available with our previous publication [10].

6.1 Matlab code u-Limits

The Matlab code *u-Limits* speeds up the processing of the collected reaction kinetics information. Once all kinetic information has been collected, the *T–f* tables and the covariance matrix of the Arrhenius parameters can be generated in a few minutes using this Matlab code, which subsequently also calls codes UBAC and JPDAP. The code provides a visualization of the process and assists selection from several possible choices.

A separate text input file is needed for each investigated reaction. The first lines of this text input file follow the format of the summary page of the NIST database [1]. This means that each line contains a literature identifier (which is the NIST squib if it exists), the temperature range ($[T_{\min},T_{\max}]$ in K units), Arrhenius parameters (ln $\{A\}$, n, E/R; units: cm, mol, s, K). These lines can be copied from the NIST summary Web pages. Information obtained from other sources has to be encoded in a similar way. Arrhenius plots referring to different bath gases (*e.g.* data belonging to reactions $H+O_2+N_2=HO_2+N_2$ and $H+O_2+Ar=HO_2+Ar$) can be joined and processed together by assuming a temperature-independent 3rd body collision efficiency of the molecules of the bath gas relative to nitrogen. The input contains the Arrhenius parameters of the selected mean rate coefficient expression and the range of temperature of the analysis.

The program at equidistant points of temperatures determines empirical uncertainty $f(T_i)$ as the larger of the two distances (on a decimal logarithmic scale) between the mean rate coefficient k^0 and the upper and lower extreme rate coefficient values (see equation (1)). This temperature interval is by default 100 K, but any other value can be defined by the user. The automatically calculated $f(T_i)$ values can be manually revised by the user. Such corrections are needed when the automatically determined f values are unrealistically small in a temperature range, which may happen, if in this temperature range all available (typically few) data points are close to the mean

curve. Another way of manual intervention is omitting those rate coefficients that unrealistically widen the band of uncertainty. For many elementary reactions, the oldest measurements provided rate coefficient values that are very far from the recently accepted values. Usually, the initially applied experimental method was later superseded by newer techniques, which known to have smaller systematic error. In such cases the values obtained by obsolete methods are not considered at the determination of the uncertainty ranges. These data are not deleted from the input text file, but are flagged as not used ones. The automatically generated f values together with these manual corrections provide the $f_{\mathrm{original}}(T_i)$ uncertainty parameter values.

The Matlab code *u-Limits* prepares the input text files for Fortran codes UBAC and JPDAP, runs these codes, and visualizes their results. One of the generated plots shows the $f_{\mathrm{original}}(T_i)$ points, and the $f_{\mathrm{extreme}}(T)$ and $f_{\mathrm{prior}}(T)$ functions determined by codes UBAC and JPDAP. Another generated figure is an Arrhenius plot that shows all considered κ *vs.* $1/T$ functions, together with the mean line, and the upper and lower uncertainty limits calculated from $f_{\mathrm{prior}}(T)$. This allows the user to check if the determined uncertainty range of Arrhenius parameters is consistent with all data considered.

6.2 Program UBAC

Fortran code UBAC (the acronym for Uncertainty Band of Arrhenius Curves) first determines a band of possible Arrhenius curves going between the symmetric limits around the mean Arrhenius curve, defined by the $f_{\mathrm{original}}(T_i)$ values at n_T temperatures and the limits in n. Based on the symmetrically located boundaries of the Arrhenius curves, a continuous $f_{\mathrm{extreme}}(T)$ function can be defined by their distance from the mean curve for all temperatures in the interval. The Arrhenius curves of extreme parameter sets, which define the boundaries of all possible Arrhenius curves and the convex hull of their parameters, will go through at least 3 (or 2) points of the lower and upper uncertainty boundaries of κ defined in equation (3). Therefore, taking all the 3- (or 2-) combinations of n_T temperatures, and selecting either the high or the low boundary ($\kappa^0(T_\mathrm{i}) \pm f(T_\mathrm{i})\cdot\ln 10$), several Arrhenius curves can be determined and plotted. We discard all the curves, which go outside the allowed ranges at any of the n_T–3 (or n_T–2) temperatures. For Arrhenius expressions containing parameter n, those curves are also discarded which have value n outside the user defined range of $[n_{\mathrm{low}}, n_{\mathrm{high}}]$. Therefore, further limiting Arrhenius curves might be obtained by investigating curves which are hitting one of the boundaries in n and going

through boundaries in κ only at two temperatures. Symmetric limiting values $n_{low}=n^0-\Delta n$ and $n_{high}=n^0+\Delta n$ are recommended (see equation (4)) to preserve the symmetry of uncertainty domain of Arrhenius parameters and thereby leave mean values equal to the central values (see Appendix 1).

6.3 Program JPDAP

Fortran code JPDAP (the initialism for Joint Probability Density of Arrhenius Parameters) has been announced earlier [10] without a description of the numerical method applied. The code allows the determination of the covariance matrix of the Arrhenius parameters by fitting equation (7) to the uncertainty parameter values $f_{extreme}(T_i)$. Consideration of the constraints makes the direct fitting a formidable task and even advanced codes for constrained least-squares fitting like EASY-FIT Express [42] usually fail to converge. In code JPDAP the constraints are taken into account in an indirect way by reformulating equation (7) using new, unconstrained parameters (see Appendix 3) and a simplex algorithm is used for the fitting [43].

Code JPDAP determines the covariance matrix of the three Arrhenius parameters α, n, ε, or those of two Arrhenius parameters (α, ε or α, n). The codes requires that the f parameter values be known at least at 6 or 3 temperatures for the 3 or 2 Arrhenius parameter cases, respectively.

6.4 Program SAMAP

Code SAMAP can generate sets of Arrhenius parameters according to either normal or uniform distributions, using real random numbers, random numbers with Latin Hypercube sampling and Sobol' sequences. For the discussion of the features of these quasi-random numbers we refer to the recent book of Turányi and Tomlin [37]. The required inputs are the mean values and the covariance matrix of the Arrhenius parameters, the type of distribution, the temperature interval of validity, the n limits, and the required number of samples. The outputs are sets of Arrhenius parameters that follow either normal or uniform distribution and provide κ values strictly within the uncertainty limits defined by $f_{prior}(T)$ for the given temperature interval.

7 Uncertainty evaluations of the elementary reactions of H_2 and syngas combustion

7.1 Selection of the elementary reactions to be investigated

As a part of a project to investigate the performance of several recently published mechanisms for the combustion of hydrogen [44] and syngas (also called wet CO) [45], our aim was to collect all experimental data that have ever been used for testing these mechanisms. The experimental papers usually contain one or several datasets. In these datasets usually one experimental parameter is changed systematically, while the other experimental circumstances are kept fixed. A large set of experimental data was accumulated [44] for hydrogen combustion: ignition measurements in shock tubes (770 data points in 53 datasets) and rapid compression machines (229/20), concentration–time profiles in flow reactors (389/17), outlet concentrations in jet-stirred reactors (152/9) and flame velocity measurements (631/73), covering wide ranges of temperature T (890 K to 2550 K), pressure p (0.23 atm to 87 atm) and equivalence ratio φ (0.1–5.6). Also, a large amount of experimental data was collected [45] for syngas combustion: ignition studies in shock tubes (732 data points in 62 datasets) and rapid compression machines (492/47), flame velocity determinations (2116/217) and species concentration measurements from flow reactors (1104/58), shock tubes (436/21) and jet-stirred reactors (90/3). These experimental datasets also cover wide ranges of temperature T (700 K to 2870 K), pressure p (0.5 atm to 450 atm), equivalence ratio φ (0.1–6.8) and CO/H_2 ratio (0.05–243).

All data were encoded in PrIMe format [46]. A custom made Matlab code called Optima [19] was used for carrying out simulations at each experimental condition. Code Optima reads the PrIMe datafile, created the input file of the corresponding CHEMKIN-II simulation code (SENKIN, PREMIX or PSR), ran the simulations using the recent mechanism of Kéromnès *et al.* [47], carried out local sensitivity analysis, and processed the results. This way the top ten most influential reactions at each experimental condition were identified. The 22 reactions steps discussed in this paper (see Table 2) are the union of the top ten most influential reactions at all conditions. Those reaction steps that appeared in the top ten only in a few experimental data points were not included in the 22 selected reactions. This procedure ensured that the most influential reaction steps under the majority of experimental conditions published in the literature were identified.

7.2 Protocol for data collection and evaluation

For the investigation of the uncertainty of the rate parameters of each elementary reaction, the data were collected by strictly following the protocol below:

1. Using the NIST Chemical Kinetics Database [1], data for the experimental and theoretical determinations of the rate coefficients were collected for both directions of the elementary reaction. The direction associated with more rate information was considered as the forward one. High-pressure and low-pressure limits were handled separately. The uncertainty of the parameters of pressure dependence (*e.g.* Troe parameters) was not investigated.
2. Evaluated kinetics data were collected from several reviews. These reviews also suggested original articles on experimental measurements and theoretical calculations that were not referenced in the NIST database. Direct experimental determinations and theoretical results, discussed in the reviews and not present in the NIST web site were added to our data collection. The starting point was the latest evaluation of Baulch *et al.* [8]. The following recent review articles about hydrogen combustion were also considered: Ó Conaire *et al* . [48], Konnov [9], Hong *et al.* [49] , Burke *et al.* [50], and Kéromnès *et al.* [47] . Several of these reviews (Konnov [9], Hong *et al.* [49] and Burke *et al.* [50]) also contain a detailed discussion about the experimental and theoretical determinations of the rate coefficient values. For the reactions of the carbon-containing species, the following review and modelling articles were considered: Mueller *et al.* [51], Davies *et al.* [15], Li *et al.* [52] , Sun *et al.* [53] and Kéromnès *et al.* [47].
3. The Arrhenius parameters of the backward reactions were converted to those of the forward reactions using equations (13), (14), (15), (16) with the help of program MECHMOD [54]. The required thermodynamic data (enthalpies and entropies of formation) for the calculations were taken from Kéromnès *et al*. [47]. The original forward parameters and those obtained from the reverse direction measurements were used together for data evaluation.
4. Using all the information above, separate tables of Arrhenius parameters were created for each elementary reaction based on the reviews, measurements and theoretical papers. If the rate coefficient depended on 3rd body efficiencies, then the corresponding series of tables were set up also for each bath gas. In these tables, the rate parameters were always given for the forward reaction and a note indicated if the parameters had been calculated from the data of the backward reaction. In this latter case, we also estimated the increase of the uncertainty using equation (9). In all cases we found that for the species of the hydrogen and syngas

combustion systems the uncertainty of the thermodynamic data is low, therefore the uncertainty of the backward reaction can be considered to be equal to the uncertainty of the forward reaction. This may not be the case for other combustion systems, when the fuel is a larger molecule. Separate tables contained the original Arrhenius parameters determined for the backward reaction, allowing the checking of the corresponding information in the main tables.

5. Third body collision efficiency parameters were collected for all bath-gas-dependent rate coefficients. In all cases, the collision efficiency of nitrogen was considered to be unity and all other collision efficiencies were related to this. Some reviews and other literature sources define separate Arrhenius parameters for different bath gases. Plotting the ratio of these rate coefficients as a function of temperature (*e.g.* plotting $m(T) = k(\mathrm{Ar},T) / k(\mathrm{N_2},T)$) usually indicates that collision efficiency m changed little in the whole temperature range. In this work we always assumed temperature independent third body collision efficiencies. The relative collision efficiencies are summarized in a table that contains information for bath gases H_2O, H_2, Ar, He, O_2, CO, and CO_2. This table indicates the mean value of the relative collision efficiency, a reasonable conservative range of collision efficiencies and the collision efficiencies as used in the various articles. Due to the scarcity of the 3rd body collision efficiency information, the mean value and the range of uncertainty were determined in an arbitrary, but conservative way and these values were not results of data evaluation. The rate information obtained for different bath gases were combined using the indicated mean relative collision efficiency values.
6. A mean rate coefficient–temperature function $\kappa^0(T)$ was selected. For most of the reactions, this mean value was identical to the Baulch *et al.* [8] recommendation. In other cases, another literature $\kappa(T)$ was selected that runs approximately halfway between the upper and lower extremes of the literature values. It has to be emphasized that $\kappa^0(T)$ is the mean curve of the uncertainty band and not a new evaluated rate coefficient. This work does not aim to recommend new evaluated rate coefficient–temperature functions and the selected set of Arrhenius parameters should not be interpreted in this way.
7. For some of the reactions, the temperature dependence of the rate coefficient is defined by a double Arrhenius expression. If this temperature dependence could be equally well described by a single Arrhenius expression, then the latter was selected as the mean value. If a double Arrhenius expression was needed, the combustion temperature range (700–2500 K) was usually controlled by one of the two sets of Arrhenius parameters. In this case the $k^0(T)$

function was the sum of the two Arrhenius expressions, but the calculated uncertainty domain was attributed to the Arrhenius expression that are dominant in the combustion temperature range. In our investigations two reactions (R13 and R19) belonged to this category.

8. The temperature interval [T_{min}, T_{max}] was usually defined as 700–2500 K. In this temperature range, $f_{original}$ values were determined equidistantly at every ΔT using the program *u-Limits* in such a way that all considered experimentally determined or theoretically calculated $\kappa(T)$ functions remained between $\kappa_{min}(T)$ and $\kappa_{max}(T)$ curves. Usually ΔT=100 K was used. Program UBAC was used to process $f_{original}$ values in order to determine uncertainty parameter values $f_{extreme}$ at every 100 K, which are consistent with the Arrhenius expression in the whole temperature interval.
9. The $f_{extreme} - T$ data pairs were used for the determination of the parameters (standard deviations and correlations) of the covariance matrix of the Arrhenius parameters by program JPDAP. The $f_{prior}(T)$ curve was then calculated from the covariance matrix obtained.
10. For several important elementary combustion reactions many experimental and theoretical determinations are available. For these elementary reactions, multivariate normal distributions of the Arrhenius parameters are assumed. In our studies, 13 reactions (R1–R4, R6–R12, R15–R16) belonged to this category.
11. For many elementary reactions very little chemical kinetics information is available. The data evaluations used usually recommended a temperature-independent uncertainty parameter f. In this case all the three uncertainty functions were the same ($f_{original}(T)=f_{extreme}(T)=f_{prior}(T)$), and $\sigma_\alpha = f \times (\ln 10)/3$, while all other parameters of the covariance matrix were zero. Uniform distributions of the Arrhenius parameters among their limits can be assumed in this case. In our investigations, 8 elementary reactions (R5, R13, R14, R17–R20, R22) belonged to this group.
12. If the rate coefficient of an elementary reaction does not change with temperature and the rate coefficient has been determined in many investigations, then a normal distribution for κ can be assumed, which implies the same normal distribution for α. In this case $f_{original}=f_{extreme}=f_{prior}$ and all parameters of the covariance matrix are zero, except for $\sigma_\alpha = f \times (\ln 10)/3$. This is the case of reaction R21 in our studies.

(a)

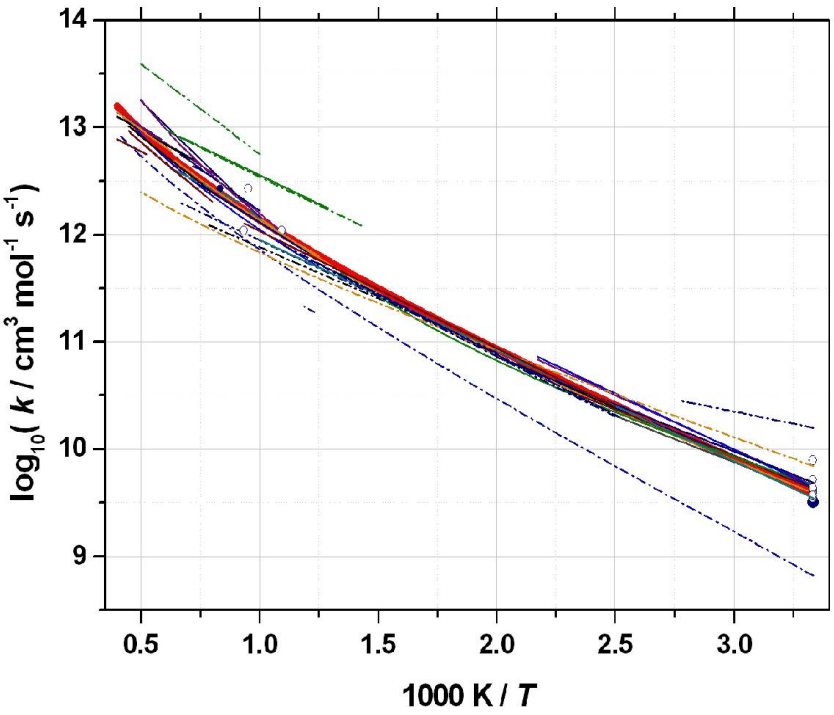
14
13
12
11
10
9
0.5
1.0
1.5
2.0
2.5
3.0
log10(k / cm3 mol-1 s-1)
1000 K / T

(b)

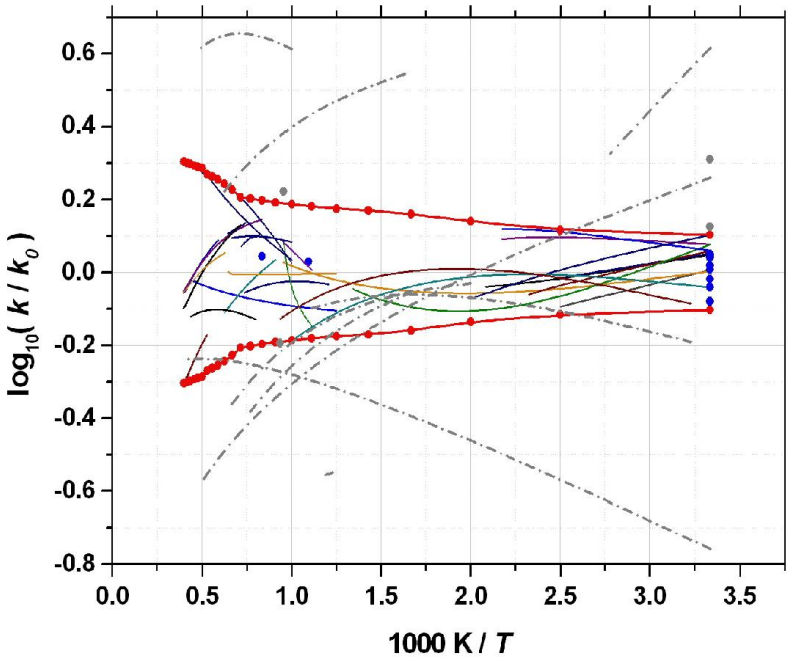
0.6
0.4
0.2
0.0
-0.2
-0.4
-0.6
-0.8
0.0
0.5
1.0
1.5
2.0
2.5
3.0
3.5
log10(k / k0)
1000 K / T

(c)

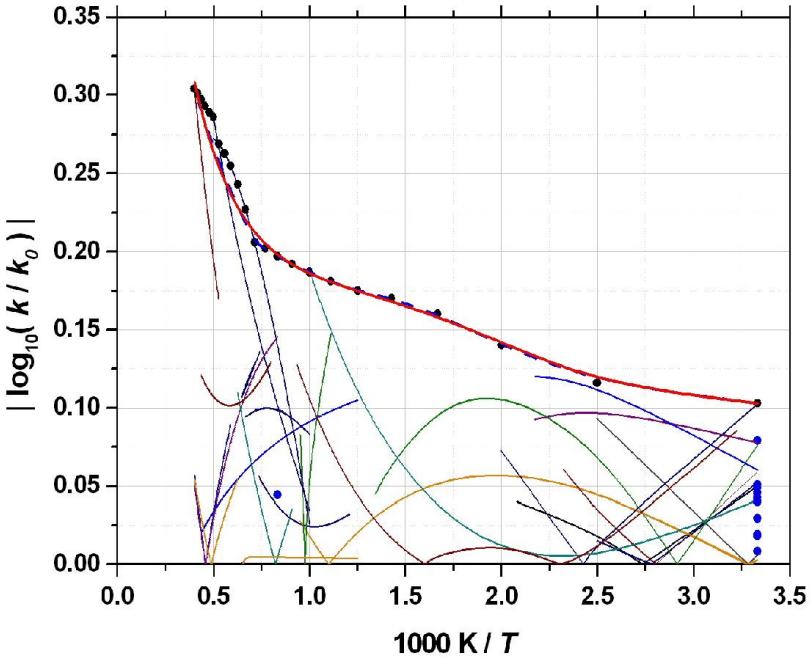

Fig. 4. (a) Arrhenius plot of the rate coefficient of reaction R4: OH + H_2→ H_2O + H. All measured and theoretically suggested rate coefficients found in the literature are shown. The mean curve is indicated with thick red line. (b) The previous figure was transformed in such a way that at each temperature the mean $\log_{10}\{k^0\}$ was subtracted from the measured or theoretically calculated $\log_{10}\{k\}$ values. As a result of the transformation, $\log_{10}\{k/k^0\}$ was plotted as a function of 1000 K/T. Some of the rate coefficient functions were far from the band determined by the others. These are indicated by grey dash-dotted lines and grey dots, and not considered at the determination of the uncertainty band. The latter is represented as f_{original} points at every 100 K interconnected with lines. (c) Taking the absolute values of the not rejected rate coefficient functions plotted in (b), the relation of the uncertainty parameters and the experimental (or theoretical) rate coefficient expressions is depicted. The black dots indicate f_{original} points, the dashed line the f_{extreme} function, while the solid red line the f_{prior} function.

Transformation of the Arrhenius plot of all literature rate coefficient expressions to the uncertainty band is illustrated in Fig. 4 on the example of reaction R4: OH + H_2→ H_2O + H. All collected measured and theoretically suggested rate coefficient expressions are given in the Supplementary and these are depicted in an Arrhenius plot in Fig. 4a. The selected mean rate expression was originally suggested by Baulch *et al*. [8]. Fig (b) shows $\log_{10}\{k/k^0\}$ as a function of 1000 K/T, where k^0 is the mean rate coefficient value and the k values are calculated by the rate expressions suggested in the literature. This is equivalent to the calculation of the difference

of $\log_{10}\{k\}$ and the mean $\log_{10}\{k^0\}$. This figure also contains the f_{original} points at every 100 K. In the low (300 K to 450 K) and high (900 K to 2500 K) temperature regions the f_{original} points closely follow the extreme $\log_{10}\{k/k^0\}$ values. In the middle temperature range (450 K to 900 K) the f_{original} points interpolate the high uncertainty of the neighbouring temperatures to avoid the suggestion of unrealistically low uncertainty in this region. This figure also shows that taking into account all rate coefficient expressions suggested in the literature would lead to unrealistically last uncertainty limits (about f=0.7). The not considered rate coefficient expressions are indicated by grey dash-dotted lines in Fig. 4 (b) and are denoted by non-bold characters in the corresponding table of the Supplementary. Finally, Fig. 4 (c) shows the absolute values of the $\log_{10}\{k/k^0\}$ functions and their relation to the f_{original}, f_{extreme} and f_{prior} uncertainty parameter functions.

All the tables and figures obtained using the protocol above are provided in the Supplementary Material. A series of tables was produced for each elementary reaction containing information on the rate coefficients (see step 4) and possibly the 3rd body collision efficiency parameters (see step 5). To support the applicability of the content of the tables, reference is made to the original reaction numbering of the review and modelling papers, and page numbers in the Baulch *et al.* [8] review. At the end of each section for a given reaction, the uncertainty parameter $f_{\text{original}}(T_i)$ obtained from the overview of the literature, is tabulated in every 100 K within the temperature range of evaluation. The information of the tables is visualized in a series of figures. The first figure is an Arrhenius plot that shows all reviewed, measured, and calculated rate coefficients that were used in the determination of the uncertainty limits. The corresponding rows of the tables are printed in bold. This figure also shows the mean curve, and the upper and lower uncertainty limits, calculated from the covariance matrix of the Arrhenius parameters. The next figure presents the tabulated $f_{\text{original}}(T_\text{i})$ points together with $f_{\text{extreme}}(T)$ and the $f_{\text{prior}}(T)$ function. Finally, a table provides the parameters of the calculated covariance matrix (*e.g.* σ_α, σ_n, σ_ε, $r_{\alpha n}$, $r_{\alpha\varepsilon}$, $r_{n\varepsilon}$ for a three-parameter Arrhenius expression), the temperature range of validity and, for a quick assessment, also the minimum and maximum values of the uncertainty parameter f_{prior} in this temperature range. Comparing these values with the uncertainty parameters published in the literature, the $f_{\text{prior}}(T)$ values recommended here are usually equal to or slightly higher, since we always provide a safe upper estimate for the uncertainty of the rate coefficients at the investigated temperatures.

7.3 Discussion of the uncertainty information for each reaction step

Reaction R1: H + O_2 = O + OH

This is the main chain branching reaction in hydrogen and syngas combustion systems, and also in the high temperature oxidation of hydrocarbons. A large amount of experimental data is available for both the forward and backward directions. The rate coefficient is known with low uncertainty: Baulch *et al.* [8] and Konnov [9] indicated f=0.10–0.18 uncertainty. Hong *et al.* recently measured [55] the rate coefficient in the temperature range 1100 – 3370 K and they reported a 10% (2σ) experimental uncertainty (about f=0.04). Burke *et al.* [50] also recently reviewed this rate coefficient and basically accepted the Hong *et al.* parameters. However, the calculated ignition delay times and flame velocities are so sensitive to this rate coefficient, that this relatively small uncertainty causes high scatter in the simulation results. Our mean rate expression is the Baulch *et al.* recommendation, the estimated uncertainty is f=0.21 at 1300 K and increases to both lower temperatures (f= 0.29 at 800 K) and higher temperatures (f= 0.33 at 2700 K).

Reaction R2: H + O_2 + M = HO_2 + M (low-pressure limit)

This reaction converts the highly reactive H atom to the low reactivity HO_2 radical. Selection of the rate coefficients of reactions R1 and R2 have high influence on the calculated flame velocities and ignition delay times of hydrogen, syngas and hydrocarbon oxidation systems. In atmospheric combustion systems and up to moderate pressures, the rate coefficient is determined by the low-pressure limit, therefore only that uncertainty is investigated here. In accordance with its high importance, several direct measurements are available, mainly with argon and nitrogen bath gases, but some measurements with water and helium bath gases are also available. Baulch *et al.* [8] and Konnov [9] suggest uncertainty parameter f=0.08–0.3 for the various bath gases, while our estimation changes between f=0.19 (600 K) and f=0.39 values (2000 K). Our mean rate expression is the Baulch *et al.* recommendation for bath gas N_2. Third body collision efficiencies 10.0, 0.5, and 0.6 were used for bath gases H_2O, Ar, and He, respectively, relative to the unit collision efficiency of N_2. Several reviewers recommend (α,n)-type two-parameter Arrhenius expressions and our uncertainty domain also refers to these two parameters.

Reaction R3: $O + H_2 = H + OH$

Reaction R3 is the second most important chain branching step (after R1) in several combustion systems and, accordingly, many experimental results have been published on the determination of the rate coefficient. Baulch *et al.* [8], Hong *et al.* [49] and Burke *et al.* [50] recommended double Arrhenius expressions, while Konnov [9] and Kéromnès *et al.* [47] used a single 3-parameter Arrhenius expression. We adopted the suggestion of Konnov [9] as the mean rate coefficient expression and therefore the uncertainty domain of the corresponding three Arrhenius parameters were defined. The estimated uncertainties were f= 0.20 (Baulch *et al.* [8]) and f= 0.11 (Konnov [9]). The uncertainty parameter derived here changes between f=0.15 and 0.20.

Reaction R4: $OH + H_2 = H_2O + H$

The reverse reaction converts H atoms to OH radicals and therefore the calculated flame velocity is highly sensitive to its rate coefficient at fuel-lean conditions. There are many experimental data available for the rate coefficient of the forward reaction and also some data for the backward direction. Konnov [9] suggested f=0.3, while Baulch *et al.* [8] assumed f=0.1 at 250 K, increasing to f=0.3 at 2500 K. We used the mean rate coefficient expression of Baulch *et al.* and our uncertainty limits are very close to the Baulch *et al.* [8] recommendation, that is f=0.10 at 300 K increasing almost linearly to 0.31 at 2500 K.

Reaction R5: $H_2O_2 + H = H_2 + HO_2$

A single room temperature measurement and few theoretical calculations are available. Baulch *et al.* [8] and Konnov [9] suggested significantly different rate expression compared to those of Hong *et al.* [49], Burke *et al.* [50] and Kéromnès *et al.* [47]. A temperature-independent uncertainty parameter, f= 0.5, was suggested by both Baulch *et al.* [8] and Konnov [9]. We used the rate coefficient expression of Kéromnès *et al.* [47] as the mean and, by assuming a temperature-independent uncertainty of f= 0.6, the uncertainty limits obtained include all review recommendations above 400 K.

Reaction R6: $H + HO_2 = OH + OH$

The rate coefficient of the overall reaction ($H + HO_2 \rightarrow$ products) was measured at room temperature, but the branching ratio is uncertain, especially at higher temperatures. Baulch *et al.* [8] and Konnov [9] suggested uncertainty parameters f=0.15 and f=0.3, respectively. The recommendation of Baulch *et al.* [8] is very different from the later reviews, and Konnov [9] is also slightly different from the others. Burke *et al.* [50] provided a detailed discussion of the

reaction and they also revisited the theoretical determination of its rate coefficient. Our mean line corresponds to the Kéromnès *et al.* [47] two-parameter (α,ε)-type recommendation, which is almost identical to the Hong *et al.* [49] and Burke *et al.* [50] recommendation. The suggested uncertainty limits are determined by the deviations between the rate coefficient expression of Konnov [9] and those of the others. The obtained uncertainty–temperature function was further increased by f=0.1, which resulted in the recommendation of Konnov [9] not lying at the edge of the uncertainty range. The uncertainty parameter function obtained varies from 0.28 to 0.47.

Reaction R7: H + HO_2 = H_2 + O_2

The reverse reaction of R7 is the main initiation reaction in the homogeneous explosion of hydrogen–oxygen mixtures. Baulch *et al.* [8] and Konnov [9] suggest an uncertainty parameter f=0.3. The measurements, theoretical calculations and reviews span a band with the expression of Hong *et al.* [49] in the middle. Therefore, the expression of Hong *et al.* [49] was selected as the mean, and the width of the uncertainty band was increased by f=0.1 to include all recommendations. The uncertainty parameter obtained varies between 0.28 and 0.54.

Reaction R8: HO_2 +OH = H_2O + O_2

Reaction R8 is an important chain termination reaction in flames. The reaction was recently reviewed and discussed in details by Burke *et al.* [56]. Several authors (Konnov [9], Burke *et al.* [56], Hong *et al.* [57]) recommended the application of the sum of two Arrhenius expressions, while other reviewers recommended a single 2-parameter Arrhenius expression. We investigated the uncertainty of the 2-parameter Arrhenius expression as suggested by Kéromnès *et al.* [47]. In the determination of the uncertainty range, the very low measured values of Hippler *et al.* [58] and Kappel *et al.* [59] were not considered, in accordance with the analysis of Burke *et al.* [56]. The recommendations of Baulch *et al.* [8] and Konnov [9] relied on the Hippler *et al.* and Kappel *et al.* measurements, therefore their suggestions were not considered here. The remaining measurements and reviews suggest an uncertainty band, which was further increased by f=0.1 to include all data, giving an uncertainty parameter near f=0.45. This uncertainty margin satisfactorily includes the results of all recent measurements. The mean rate expression is an (α,ε)-type two-parameter Arrhenius expression, but considering only the uncertainty of the Arrhenius parameters α and ε did not provide a good description of the $f_{\text{extreme}}(T)$ uncertainty parameter curve. Therefore, while the mean value of n was kept at zero, we assumed that it has a

nonzero uncertainty. Assuming that all the three Arrhenius parameters are uncertain allowed a good description of the shape of the uncertainty band while σ_n has a value as low as 0.32.

Reaction R9: OH + OH → H_2O_2 (high-pressure limit)

The high-pressure limit rate coefficient of reaction R9 is important only at pressures much higher than atmospheric, whereas at atmospheric pressure the reaction is close to its low-pressure limiting behaviour. The forward reaction is a sink of the OH radicals, while the reverse reaction is a key reaction for the simulation of fuel–air mixtures in engines (see the discussion by Hong *et al.* [49], who refers to Westbrook [60]) There are no experimental data at combustion temperatures, only below 800 K. Baulch *et al.* [8] recommended a high-pressure limit rate coefficient only in the temperature range of 200–400 K with an uncertainty f=0.2. Konnov [9] provided a recommendation up to 1500 K, with an uncertainty f=0.4. Hong *et al.* [49] recommended a rate coefficient for the reverse reaction in the temperature range 1000 – 1200 K with an uncertainty of 21% (f=0.08). Troe [61] reviewed this reaction in detail in both directions, and recommended parameters for the temperature and pressure dependence of the rate coefficient based on experimental results and theoretical calculations. In our calculations the rate coefficient expression of Konnov [9] was used as the mean curve. The uncertainty limits were defined to include all rate coefficients recommended in the reviews. This uncertainty parameter is 0.4 at 1000 K, increasing to 0.5 at 1500 K and 0.7 at 2000 K. The rate expression of Konnov was (α,n)-type, but the T–f points could not be reproduced by assuming that these Arrhenius parameters are uncertain only. Therefore, the activation energy E was also considered to be uncertain, and in this way the fitted $f(T)$ function is satisfactorily described the uncertainty points.

Reaction R9: OH + OH+M = H_2O_2+M (low-pressure limit)

For the bath gas N_2, Baulch *et al.* [8] recommended a rate coefficient only for the temperature range 200 – 400 K (f=0.2), while Konnov [9] provided a rate coefficient with uncertainty f = 0.4 in temperature range 250 – 1400 K. Hong *et al.* [49] recently investigated this reaction and determined a more accurate rate coefficient expression with an uncertainty of 21% (f=0.08) in range 1000 – 1460 K. Kéromnès *et al.* [47] used a slightly different expression than Hong *et al.* to describe better the indirect experimental data at high pressures. The recommendations of Konnov [9] and Baulch *et al.* [8] are very different from the recent Hong *et al.* [49] measurements, therefore these recommendations are not considered here. All remaining

measurements and reviews resulted in an uncertainty value, which was increased by 0.1 to include all the data. The obtained uncertainty parameter values $f_{prior}(T)$ are 0.35 at 800 K, increasing to 0.50 at 1000 K and 0.70 at 1900 K. The experimental data refer to bath gases N_2, Ar and H_2O. We used mean 3rd body efficiencies m(Ar) = 0.67 and $m(H_2O)$ = 8.33 relative to that of nitrogen.

Reaction R10: H + OH + M = H_2O + M (low-pressure limit)

Calculated flame velocity values are very sensitive to the rate coefficient of this recombination reaction, which is close to the low-pressure limit at all experimental conditions. There is limited number of experimental data for N_2, Ar and H_2O bath gases. Srinivasan and Michael [62] recently measured the rate coefficient at high temperatures (2196 – 3190 K) with low (18%) reported uncertainty, although these values are not in good accordance with the previous measurements. Konnov [9] suggested uncertainty f=0.3, while Baulch *et al.* [8] suggested f=0.3 for Ar and f=0.5 for N_2 and H_2O. We accepted the rate expression of Konnov [9] for N_2 bath gas as the mean one. Experimental and theoretical values for bath gases Ar and H_2O were merged with the N_2 data using relative 3rd body efficiency values m(Ar)= 0.38 and $m(H_2O)$=6.45. The reviews, and the experimental and theoretical data provide an uncertainty band with typical radius f=0.3 at 400 K increasing to f=0.63 at 2000 K.

Reaction R11: OH + OH = H_2O + O

Many experimental data in good accordance are available. Baulch *et al.* [8], Konnov [9], and Hong *et al.* [49] suggested rate coefficient expressions with low uncertainty. The f values are 0.15, 0.18 and 0.06–0.10, respectively. We accepted the expression of Baulch *et al.* [8] as our mean. The uncertainty band determined includes all the data and $f_{prior}(T)$ increases from 0.20 at 900 K to 0.32 at 2000 K.

Reaction R12: H + H + M = H_2 + M (low-pressure limit)

There are measured data with bath gases N_2, Ar, H_2, and H_2O. Most of the reviews provide different rate expressions for the different bath gases, but Kéromnès *et al.* [47] recommended a single Arrhenius expression for nitrogen and various 3rd body efficiencies for the other bath gases. Baulch *et al.* [8] recommended f = 0.5 in the case of all bath gases, while Konnov [9] considered different f values for the bath gases of Ar (0.3), N_2 (0.5), H_2 (0.4), and H_2O (0.7). We adopted the [8] recommendation of Baulch *et al.* for nitrogen as the mean value. Experimental and theoretical values for the other bath gases were merged with the N_2 data using 3rd body

efficiency values m(Ar)= 0.87, m(H_2)= 2.5 and m(H_2O)=12. These values outline an uncertainty band, which was widened by f = 0.1, giving values increasing from f=0.35 (600 K) to f=0.70 (2100 K).

Reaction R13: $HO_2 + HO_2 = H_2O_2 + O_2$

At low temperatures, this reaction proceeds via two mechanisms, one of which is pressure dependent and the other is pressure independent. There are many experimental data, but almost all these data are below 400 K. Many low-temperature measurements were carried out in nitrogen bath gas at 1 bar, in accordance with the atmospheric significance of this reaction. At combustion temperatures (above about 500 K) the pressure-independent mechanism is the dominant, and therefore the rate coefficient can be considered pressure independent. All reviewers suggest a double Arrhenius expression. Konnov [9] proposed a slightly different expression, while the recommendation of all other reviewers are identical. Plotting the Baulch *et al.* [8] recommendation (see the figure in the Supplementary Material) shows that both terms of the double Arrhenius expression are important in the temperature range of 650 – 1000 K. Above 1000 K the expression is dominated by the positive activation energy term and below 650 K it is dominated by the negative E term. Baulch *et al.* suggested f=0.15 in temperature range 550 – 800 K rising to 0.4 at 1250 K. Konnov provided separate uncertainties (f=0.15 and f=0.4) for the negative and positive activation energy expressions, respectively. Since we are interested in the uncertainty of the rate coefficient above 700 K, a temperature-independent uncertainty parameter f_{prior}= 0.4 was accepted, and the uncertainty of the Arrhenius parameters of the positive activation energy term was calculated.

Reaction R14: $H_2O_2 + H = H_2O + OH$

The few measurements available were made before 1974 and below 770 K. Both Baulch *et al.* [8] and Konnov [9] suggested uncertainty parameter f=0.3 for the temperature region 300 – 1000 K. We accepted the suggestion of Kéromnès *et al.* [47] as the mean rate expression and assumed a temperature-independent f=0.4. The corresponding uncertainty band includes all rate coefficient curves suggested in the various reviews in temperature range 300 – 2500 K.

Reaction R15: $CO + OH = CO_2 + H$

This is the most important elementary CO reaction in combustion systems, since it converts OH radicals to H atoms. Kéromnès *et al.* [47] and Davies *et al.* [15] suggested a double Arrhenius expression, while Sun *et al.* [53] recommended a triple Arrhenius expression. The reaction is

pressure dependent at low temperature, whereas at combustion temperatures it is pressure independent. The Arrhenius *A* values of Davies *et al.* [15] are optimized ones and they assumed uncertainty f=0.08. Many measurements for this rate coefficient are available. We accepted the single three-parameter Arrhenius equation suggested by Li *et al.* [63] as the mean rate expression. Assuming uncertainty parameter $f_{prior}(T)$ changing from 0.18 (1200 K) to 0.3 (2500 K), the uncertainty band includes all recent rate determinations and reviews.

Reaction R16: HCO + M = H + CO + M

This is another very important CO elementary reaction. The rate coefficient is close to the low-pressure limit even at 100 bar. There are several measurements, mainly from the 1970's for bath gases N_2, Ar, H_2, He and CO. Baulch *et al.* [8] suggested an uncertainty parameter f = 0.3 for Ar bath gas in temperature range 500 –2500 K. Davis *et al.* [15] also assumed f = 0.3 for N_2 bath gas. We accepted the rate expression suggested by Kéromnès *et al.* [47] for N_2 bath gas. The relative third body efficiencies with respect to N_2 are given in the Supplementary Material. The uncertainty parameters $f_{prior}(T)$ suggested here change from 0.32 (1000 K) to 0.56 (2200 K).

Reaction R17: CO +O_2 = CO_2 + O

Few experimental data are available in either direction, since measurement of both the forward and the reverse rate coefficients is technically difficult. Davis *et al.* [15] reported uncertainty parameter f=0.5. All reviewers except for Kéromnès *et al.* [47] used the same set of Arrhenius parameters. We accepted the Arrhenius equation that was first suggested by Mueller *et al.* [64] as the mean rate expression. A constant uncertainty parameter f_{prior}=0.7 defines a band that includes all review and experimental data.

Reaction R18: H + O + M = OH + M (low-pressure limit)

A single experimental expression is available for this rate coefficient based on the measurements of Javoy *et al.* [65]. Konnov [9] suggested f=0.5 for temperature range 2950 – 3700 K, using the estimated uncertainty of the Javoy *et al.* measurement. The 3rd body collision efficiency coefficients given in the various reviews were assigned without any experimental or theoretical background. Our mean rate coefficient expression is identical to those of Kéromnès *et al.* [47] and we assumed constant f=0.5 uncertainty parameter.

Reaction R19: $H_2O_2 + OH = HO_2 + H_2O$

This reaction is important in the intermediate-temperature ignition of hydrocarbons and alcohols. Hong *et al.* [66] recently measured the rate coefficient in the temperature range of 1020 – 1460 K. Hong *et al.* [67] also combined the obtained rate coefficients with room-temperature measurement data and described the temperature dependence of the rate coefficient in a wide range of temperatures by a double Arrhenius expression. They assigned uncertainty of 27% (f=0.10). Previously Baulch *et al.* [8] and Konnov [9] suggested uncertainty parameter f=0.5 and f=0.3, respectively, for the temperature range 800 – 1700 K. The double Arrhenius expression of Hong *et al.* [67] was also accepted by Burke *et al.* [50] and Kéromnès *et al.* [47], and we also use this rate expression as the mean one. We assigned a more cautious f_{prior}=0.3 constant in temperature range 800 – 2500 K.

Reaction R20: $HCO + O_2 = HO_2 + CO$

There are many measurements available, but mainly at room temperature and below 700 K. No reviewers have suggested an uncertainty parameter for this reaction. Most reviews and modelling studies use the experimental rate expression of Timonen *et al.* [68]. The mean rate coefficient expression used here is also based on their values and it is the identical to that of Kéromnès *et al.* [47]. We assumed constant f=0.3 uncertainty parameter, which includes most measured rate coefficients.

Reaction R21: $HCO + H \rightarrow H_2 + CO$

This is a radical–radical reaction and therefore near zero temperature dependence is expected. All reviewers suggested a single A-factor as an Arrhenius expression. The experimental data, available from 295 K to 2700 K, also indicate no temperature dependence for the rate coefficient. Baulch *et al.* [8] suggested uncertainty parameter f=0.3. We use the rate expression of Baulch *et al.* as the mean and an assumed temperature-independent f=0.5. The uncertainty band obtained includes all rate coefficient values.

Reaction R22: $CO + HO_2 \rightarrow CO_2 + OH$

This reaction is important at high pressure (above 15 bar) and low temperature (below about 1100 K), that is at the conditions of several RCM experiments [69]. Davis *et al.* [15] applied uncertainty parameter f=0.3. We use the rate expression of Kéromnès *et al.* [47] as the mean, which is based on the theoretical determination of You et al. [70]. Apart from the You *et al.*

article, very few and not recent experimental and theoretical rate determinations are available, and therefore we assumed temperature independent uncertainty f=0.7.

7.4 Summary of the uncertainty information for the investigated elementary reactions

The last paragraph of Section 7.2 described the tables and figures given in the Supplementary Material. This contains all raw information and also the derived covariance matrices and f_{prior} functions for each reaction. To facilitate the application of these results in combustion modelling, the prior uncertainty information determined for the 22 reactions are summarized also in Tables 2 and 3. The rows of Table 2 contain the chemical reactions and the mean Arrhenius parameters α, n, ε. For reactions R5, R13, R14, R17, R18, R19, R20, R21 and R22, the uncertainty is characterized by $\sigma_\alpha = f \times (\ln 10)/3$. In the case of these reactions (except for R21) a uniform probability density function is assumed. For the other reactions much more information is available, detailed in the Supplementary Material. For these reactions, uncertainty parameter values $f_{\text{original}}(T_i)$ and $f_{\text{extreme}}(T_i)$ were determined at every 100 K by programs *u-Limits* and UBAC, respectively. Using the program JPDAP, the $f_{\text{extreme}}(T_i)$ values were fitted and the parameters of the covariance matrix of the Arrhenius parameters are given in columns 7 to 12 of Table 2. Fig. 5 shows for each investigated reaction the $f_{\text{prior}}(T)$ calculated from the covariance matrix of the Arrhenius parameters.

Reactions R2, R9, R10, R12, R16, and R18 are low-pressure limit reactions. The rate parameters of these reactions correspond to the 3$^{\text{rd}}$ body collision efficiency of N_2. For these reactions, the 3$^{\text{rd}}$ body collision efficiencies for other bath gases (H_2O, H_2, Ar, He, O_2, CO, and CO_2), relative to N_2, are given in Table 3. The table indicates mean relative collision efficiencies only for those elementary reactions where the rate information for different bath gases is available.

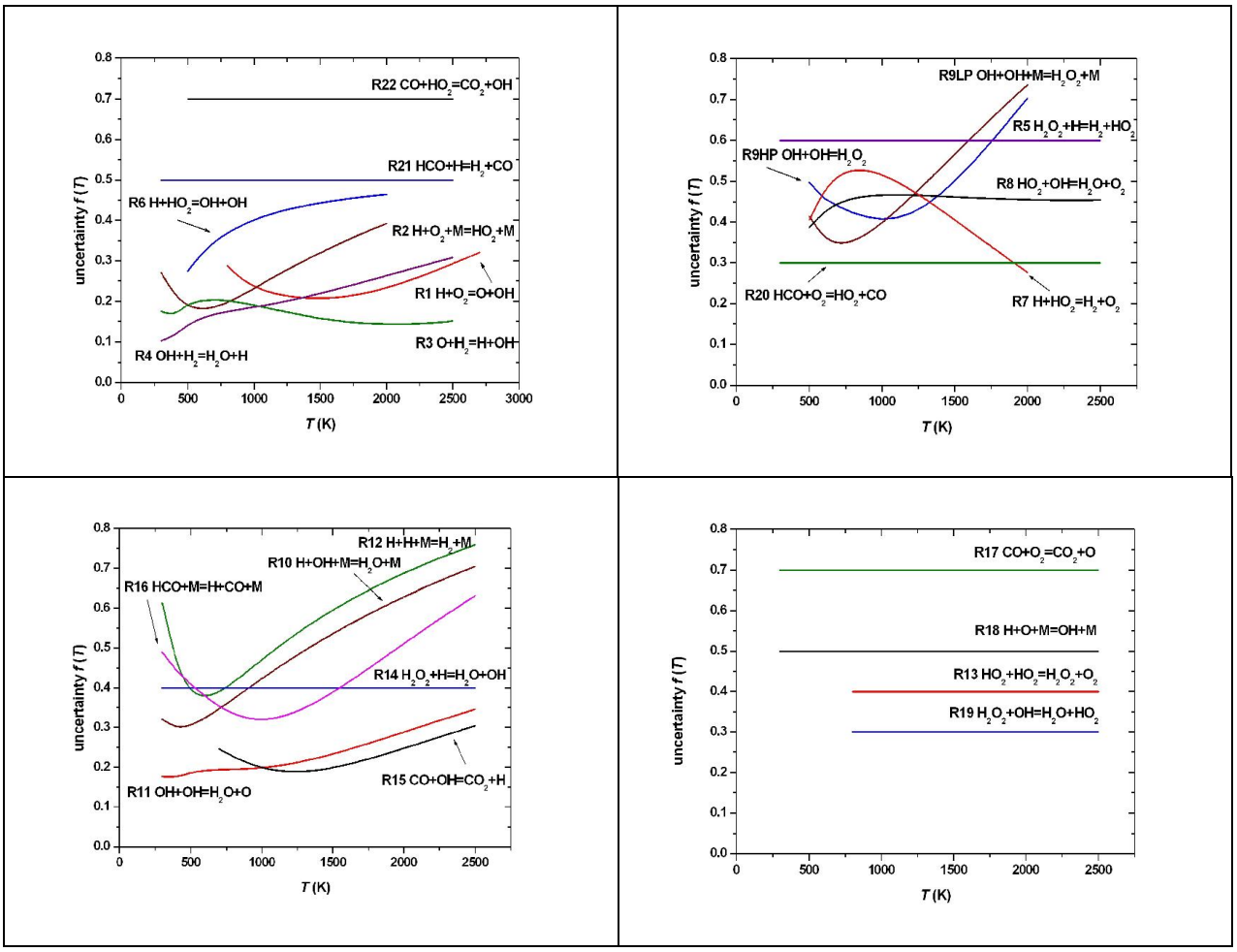

Fig. 5. Uncertainty $f_{\text{prior}}(T)$ curves for the investigated reactions.

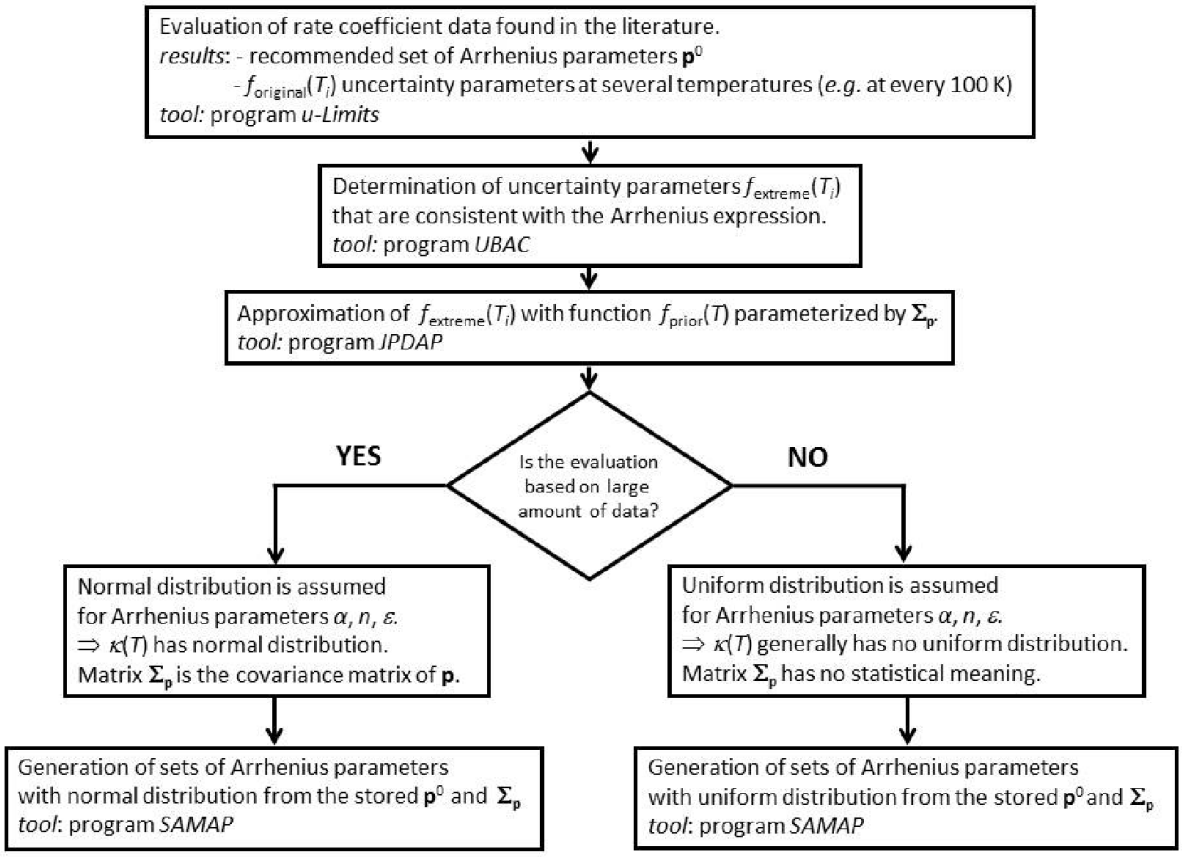

Fig. 6. Scheme for the determination of the prior uncertainty of the Arrhenius parameters

8. Conclusions

A methodology was developed for the determination and efficient storage of the domain of uncertainty of the Arrhenius parameters of gas-phase elementary reactions. First, temperature-dependent $k_{\min}$ and $k_{\max}$ values were selected at intervals of 100 K in such a way that these values provide a lower and an upper limit, respectively, of all recent measurements and theoretical determinations. Selecting a mean rate coefficient – temperature function, the limits were converted to uncertainty parameters f_{original} at every investigated temperature. This procedure was assisted by program *u-Limits*, which makes the determination of the uncertainty band a semiautomatic process. The obtained T–f_{original} data pairs may not be consistent with the temperature dependence of the rate coefficient. A calculation procedure and the corresponding computer code UBAC (the acronym of Uncertainty Band of Arrhenius Curves) was developed to

find the $f_{extreme}(T)$ curve that is consistent with the Arrhenius equation in the whole temperature interval. This curve can be used to define the domain of allowed Arrhenius parameters. The $f_{extreme}(T)$ curve can be well represented and thereby efficiently stored with the uncertainty curve $f_{prior}(T)$, which is parameterized with the covariance matrix $\mathbf{\Sigma_p}$ of the Arrhenius parameters, that has merely at most 6 non-zero parameters. The parameters of the covariance matrix can be calculated by program JPDAP (the acronym of Joint Probability Density of Arrhenius Parameters). Using program SAMAP, random sets of Arrhenius parameters having either a normal or a uniform distribution, can be generated. The rate coefficients calculated by these Arrhenius parameters are always within uncertainty limits $f_{prior}(T)$ in the whole temperature interval of evaluation. The logical structure of the procedure above is depicted in Fig. 6.

This procedure was used for the analysis of 22 important elementary reactions of the H_2 and syngas system. The collected data and the details of the calculations can be reproduced from the Supplementary Material. The summary of the numerical results and the qualitative assessment of the uncertainty of the rate coefficients of these reactions are given in the main text of the article. These data can be used for mechanism optimization and uncertainty quantification studies of hydrogen and syngas combustion models.

Acknowledgements

The authors thank the helpful discussions with Mr. Tamás Varga and acknowledge the contribution of Mr. Bence Moharos to the collection of wet CO combustion rate parameters. This work was partially financed by OTKA grant K84054.

References

1. J. A. Manion; R. E. Huie; R. D. Levin; D. R. Burgess Jr.; V. L. Orkin; W. Tsang; W. S. McGivern; J. W. Hudgens; V. D. Knyazev; D. B. Atkinson; E. Chai; A. M. Tereza; C.-Y. Lin; T. C. Allison; W. G. Mallard; F. Westley; J. T. Herron; R. F. Hampson; D. H. Frizzell NIST Chemical Kinetics Database, NIST Standard Reference Database 17, Version 7.0 (Web Version), Release 1.6.7, Data Version 2013.03, National Institute of Standards and Technology, Gaithersburg, Maryland, 20899-8320. . http://kinetics.nist.gov/
2. J. Warnatz, in: Combustion chemistry, W. C. Gardiner, (Ed.) Springer: New York, 1984; pp 197-361.
3. W. Tsang; R. F. Hampson, J. Phys. Chem. Ref. Data 15 (1986) 1087-1279
4. W. Tsang, J. Phys. Chem. Ref. Data 20 (1991) 221–273
5. W. Tsang; J. T. Herron, J. Phys. Chem. Ref. Data 20 (1991) 609-663
6. D. L. Baulch; C. J. Cobos; R. A. Cox; C. Esser; P. Frank; T. Just; J. A. Kerr; M. J. Pilling; J. Troe; R. W. Walker; J. Warnatz, J. Phys. Chem. Ref. Data 21 (1992) 411-734
7. D. L. Baulch; C. J. Cobos; R. A. Cox; J. H. Frank; G. Hayman; T. H. Just; J. A. Kerr; T. Murrels; M. J. Pilling; J. Troe; B. F. Walker; J. Warnatz, Combust. Flame 98 (1994) 59-79
8. D. L. Baulch; C. T. Bowman; C. J. Cobos; R. A. Cox; T. Just; J. A. Kerr; M. J. Pilling; D. Stocker; J. Troe; W. Tsang; R. W. Walker; J. Warnatz, J. Phys. Chem. Ref. Data 34 (2005) 757-1397
9. A. A. Konnov, Combust. Flame 152 (2008) 507-528
10. T. Nagy; T. Turányi, Int.J.Chem.Kinet. 43 (2011) 359-378
11. T. Nagy; T. Turányi, Reliability Engineering Syst. Safety 107 (2012) 29-34
12. G. Smith; D. Golden; M. Frenklach; N. Moriary; B. Eiteneer; M. Goldenberg; C. Bowman; R. Hanson; S. Song; W. Gardiner; V. lissianski; Z. Qin GRI-Mech 3.0, http://www.me.berkeley.edu/gri_mech/.
13. X. Q. You; T. Russi; A. Packard; M. Frenklach, Proc. Combust. Inst. 33 (2011) 509-516
14. X. Q. You; A. Packard; M. Frenklach, Int. J. Chem. Kinet. 44 (2012) 101-116
15. S. Davis; A. Joshi; H. Wang; F. Egolfopoulos, Proc. Combust. Inst. 30 (2005) 1283-1292
16. D. A. Sheen; X. You; H. Wang; T. Løvås, Proc. Combust. Inst. 32 (2009) 535-542
17. D. Sheen; H. Wang, Combust. Flame 158 (2011) 645-656
18. D. A. Sheen; H. Wang, Combust. Flame 158 (2011) 2358–2374
19. T. Turányi; T. Nagy; I. G. Zsély; M. Cserháti; T. Varga; B. T. Szabó; I. Sedyó; P. T. Kiss; A. Zempléni; C. H. J., Int. J. Chem. Kinet. 44 (2012) 284-302
20. I. G. Zsély; T. Varga; T. Nagy; M. Cserháti; T. Turányi; S. Peukert; M. Braun-Unkhoff; C. Naumann; U. Riedel, Energy 43 (2012) 85-93
21. T. Varga; I. G. Zsély; T. Turányi; T. Bentz; M. Olzmann, Int. J. Chem. Kinet. 46 (2014) 295–304
22. T. Varga; T. Nagy; C. Olm; I. G. Zsély; R. Pálvölgyi; É. Valkó; G. Vincze; M. Cserháti; H. J. Curran; T. Turányi, Proc. Combust. Inst. in press, doi:10.1016/j.proci.2014.06.071 (2015)
23. D. A. Sheen; C. M. Rosado-Reyes; W. Tsang, Proc. Combust. Inst. 34 (2013) 527-536
24. A. S. Tomlin, Proc. Combust. Inst. 34 (2013) 159-176
25. M. J. Brown; D. B. Smith; S. C. Taylor, Combust. Flame 117 (1999) 652-656
26. T. Turányi; L. Zalotai; S. Dóbé; T. Bérces, Phys. Chem. Chem. Phys 4 (2002) 2568-2578
27. I. G. Zsély; J. Zádor; T. Turányi, Proc. Combust. Inst. 30 (2005) 1273-1281
28. J. Zádor; I. G. Zsély; T. Turányi; M. Ratto; S. Tarantola; A. Saltelli, J. Phys. Chem. A 109 (2005) 9795-9807
29. J. Zádor; I. G. Zsély; T. Turányi, Reliab. Eng. Syst. Saf. 91 (2006) 1232-1240
30. I. G. Zsély; J. Zádor; T. Turányi, Int. J. Chem. Kinet. 40 (2008) 754-768

31. A. S. Tomlin, Reliab. Eng. Syst. Safety 91 (2006) 1219-1231
32. T. Ziehn; A. S. Tomlin, Int. J. Chem. Kinet. 40 (2008) 742-753
33. M. Cord; B. Sirjean; R. Fournet; A. Tomlin; M. Ruiz-Lopez; F. Battin-Leclerc, J. Phys. Chem. A 116 (24) (2012) 6142-6158
34. É. Hébrard; A. S. Tomlin; R. Bounaceur; F. Battin-Leclerc, Proc. Combust. Inst. in press, http://dx.doi.org/10.1016/j.proci.2014.06.027 (2015)
35. International vocabulary of metrology - Basic and general concepts and associated terms (VIM), in *http://www.bipm.org/* JCGM 200 (2008)
36. M. J. Pilling; P. W. Seakins, Reaction Kinetics, Oxford University Press, Oxford, 1995
37. T. Turányi; A. S. Tomlin, Analysis of Kinetic Reaction Mechanisms, Springer, 2014
38. B. Ruscic; R. E. Pinzon; M. L. Morton; G. von Laszevski; S. J. Bittner; S. G. Nijsure; K. A. Amin; M. Minkoff; A. F. Wagner, J. Phys. Chem. A 108 (2004) 9979-9997
39. B. Ruscic, Int. J. Quantum Chem. (2014) DOI: 10.1002/qua.24605
40. A. G. Császár; T. Furtenbacher, Chem. Eur. J. 16 (2010) 4826-4835
41. http://garfield.chem.elte.hu/Combustion/Combustion.html
42. K. Schittkowski, EASY-FIT Express, Version 1.0, in *http://num.math.uni-bayreuth.de/~kschittkowski/easy_fitx.htm* (2009)
43. J. A. Nelder; R. Mead, Computer Journal 7 (1965) 308–313
44. C. Olm; I. G. Zsély; R. Pálvölgyi; T. Varga; T. Nagy; H. J. Curran; T. Turányi, Combust. Flame 161 (2014) 2219-2234
45. C. Olm; I. G. Zsély; T. Varga; H. J. Curran; T. Turányi, Combust. Flame submitted (2014)
46. M. Frenklach, PrIMe Database, http://www.primekinetics.org/.)
47. A. Kéromnès; W. K. Metcalfe; K. Heufer; N. Donohoe; A. Das; C. J. Sung; J. Herzler; C. Naumann; P. Griebel; O. Mathieu; M. C. Krejci; E. L. Petersen; W. J. Pitz; H. J. Curran, Combust. Flame 160 (2013) 995-1011
48. M. Ó Conaire; H. J. Curran; J. M. Simmie; W. J. Pitz; C. K. Westbrook, Int. J. Chem. Kinet. 36 (2004) 603-622
49. Z. Hong; D. Davidson; R. Hanson, Combust. Flame 158 (2011) 633-644
50. M. Burke; M. Chaos; Y. Ju; F. L. Dryer; S. Klippenstein, Int. J. Chem. Kinet. 44 (2012) 444-474
51. M. A. Mueller; T. J. Kim; R. A. Yetter; F. L. Dryer, International Journal of Chemical Kinetics 31 (1999) 113-125
52. J. Li; Z. Zhao; A. Kazakov; M. Chaos; F. L. Dryer; J. J. J. Scire, Int. J. Chem. Kinet. 39 (2007) 109-136
53. H. Sun; S. I. Yang; G. Jomaas; C. K. Law, Proc. Combust. Inst. 31 (2007) 439-446
54. T. Turányi Mechmod v. 1.4: Program for the transformation of kinetic mechanisms. http://garfield.chem.elte.hu/Combustion/Combustion.html
55. Z. Hong; R. D. Cook; D. F. Davidson; R. K. Hanson, J. Phys. Chem. A 114 (2010) 5718
56. M. P. Burke; S. J. Klippenstein; L. B. Harding, Proc. Combust. Inst. 34 (2013) 547-555
57. Z. Hong; K. Y. Lam; R. Sur; S. Wang; D. F. Davidson; R. K. Hanson, Proc. Combust. Inst. 34 (2013) 565-571
58. H. Hippler; H. Neunaber; J. Troe, J. Chem. Phys. 103 (1995) 3510-3516
59. C. Kappel; K. Luther; J. Troe, PCCP 4 (2002) 4392-4398
60. C. K. Westbrook, Proc. Combust. Inst. 28 (2000) 1563-1577
61. J. Troe, Combust. Flame 158 (2011) 594–601
62. N. K. Srinivasan; J. V. Michael, Int. J. Chem. Kinet. 38 (2006) 211-219 10.1002/kin.20172.
63. J. Li; Z. Zhao; A. Kazakov; M. Chaos; F. L. Dryer; J. J. Scire, Int. J. Chem. Kinet. 39 (2007) 109–136

64. M. A. Mueller; R. A. Yetter; F. L. Dryer, Int. J. Chem. Kinet. 31 (1999) 705-724
65. S. Javoy; V. Naudet; S. Abid; C. E. Paillard, Experimental Thermal and Fluid Science 27 (2003) 371-377
66. Z. Hong; R. D. Cook; D. F. Davidson; R. K. Hanson, J. Phys. Chem. A 114 (2010) 5718-5727
67. Z. Hong; D. F. Davidson; R. K. Hanson, Combust. Flame 158 (2011) 633-644
68. R. S. Timonen; E. Ratajczak; D. Gutman, J. Phys. Chem. 92 (1988) 651-655
69. G. Mittal; C. J. Sung; M. Fairweather; A. S. Tomlin; J. F. Griffiths; K. J. Hughes, Proc. Comb. Inst. 31 (2007) 419-427
70. X. Q. You; H. Wang; E. Goos; C. J. Sung; S. J. Klippenstein, J. Phys. Chem. A 111 (2007) 4031-4042

Appendix 1: *Convexity and symmetry of the uncertainty domain of Arrhenius parameters*

This Appendix shows that the uncertainty domain of the Arrhenius parameters is always convex for both the 2-parameter and the 3-parameter Arrhenius expression cases. Also, it is proved that if the minimal and maximal $\kappa(T)$ curves are symmetric around $\kappa^0(T)$, then the uncertainty domain will also be symmetric around the mean set of Arrhenius parameters.

The uncertainty domains defined for the rate coefficients at the three sampling temperatures are intervals, which are convex in 1D. The direct product of these intervals defines a rectangular box, which is a 3D domain and also convex:

$$[\kappa_{\text{low}}(T_1),\kappa_{\text{high}}(T_1)]\times[\kappa_{\text{low}}(T_2),\kappa_{\text{high}}(T_2)]\times[\kappa_{\text{low}}(T_3),\kappa_{\text{high}}(T_3)] \tag{A1}$$

Convexity of a domain means that all line segments connecting any two points of the domain go within the domain:

$$\boldsymbol{\kappa}_x = (1-x)\boldsymbol{\kappa}_{\text{low}} + x\boldsymbol{\kappa}_{\text{high}} \qquad (0 \le x \le 1) \tag{A2}$$

A point of a line segment between points $\boldsymbol{\kappa}_{\text{low}} = (\kappa_{\text{low},1},\kappa_{\text{low},2},\kappa_{\text{low},3})$ and $\boldsymbol{\kappa}_{\text{high}} = (\kappa_{\text{high},1},\kappa_{\text{high},2},\kappa_{\text{high},3})$ in the $\boldsymbol{\kappa}$ = ($\kappa(T_1)$, $\kappa(T_2)$, $\kappa(T_3)$) space automatically fulfils the uncertainty constraints in $\boldsymbol{\kappa}$, since each of its components for i= 1, 2, 3 fulfils it. This uncertainty constraint is $-f_i \le \left(\kappa_{xi}-\kappa_i^0\right)/\ln 10 \le +f_i$ for i=1, 2, 3.

The transformation between the $\boldsymbol{\kappa}$ and $\mathbf{p}$ spaces is linear, since it requires the solution of the following system of linear equations:

$$\begin{bmatrix}\kappa(T_1)\\ \kappa(T_2)\\ \kappa(T_3)\end{bmatrix} = \begin{bmatrix}1 & \ln T_1 & -T_1^{-1}\\ 1 & \ln T_2 & -T_2^{-1}\\ 1 & \ln T_3 & -T_3^{-1}\end{bmatrix}\begin{bmatrix}\alpha\\ n\\ \varepsilon\end{bmatrix} \tag{A3}$$

A shorter notation for the equation above is $\boldsymbol{\kappa}=\mathbf{T}\mathbf{p}$. Accordingly, the Arrhenius parameter vector can be calculated from the $\kappa(T_i)$ values given at three different temperatures as $\mathbf{p}=\mathbf{T}^{-1}\boldsymbol{\kappa}$. Multiplying the terms of equation (A2) with matrix $\mathbf{T}^{-1}$ gives:

$$\mathbf{T}^{-1}\boldsymbol{\kappa}_x = (1-x)\mathbf{T}^{-1}\boldsymbol{\kappa}_{\text{low}} + x\mathbf{T}^{-1}\boldsymbol{\kappa}_{\text{high}} \tag{A4}$$

It can be written as:

$$\mathbf{p}_x = (1-x)\mathbf{p}_{\text{low}} + x\mathbf{p}_{\text{high}} \tag{A5}$$

Due to the convexity of the 3D interval in $\boldsymbol{\kappa}$, the calculated Arrhenius parameter set $\mathbf{p}_x$ will also be within the uncertainty domain of $\mathbf{p}$, which implies that this domain is also convex.

Uncertainty limits at other temperatures will impose linear inequality constraints on the $\kappa(T_i;\mathbf{p})$ values (see equation (3)), which correspond to linear inequality constraints for parameters $\mathbf{p}$ due to the linear relationship between κ and $\mathbf{p}$ (see equation (2)). These linear inequality constraints define half-spaces in $\mathbf{p}$, which correspond to truncation of the uncertainty domain by planes. The predefined limits for n are also linear inequality constraints (see equation (4)). Linear inequality constraints truncate the domain of a uniform distribution by planes, but do not affect convexity and evenness (see Appendix 2). The consequence is that while the extreme Arrhenius curves define the boundaries of the uncertainty domain of the Arrhenius curves, their parameters correspond to the vertices of the complex hull of the uncertainty domain of the Arrhenius parameters.

The uncertainty boundaries in κ are located symmetrically around the mean value at any three temperatures, therefore the constraints imposed by them in the space of parameters $\mathbf{p}$ will be also be symmetric with respect to mirroring through $\mathbf{p}^0$ due to the linear relationship between the spaces. Furthermore, applying symmetric constraints for n around n^0 also will not affect the mirror symmetry of the uncertainty domain (see Appendix 2) around the central values, therefore mirror-symmetric multivariate distributions will lead to mean values $\overline{\mathbf{p}}$ which are equal to the central values $\mathbf{p}^0$.

Appendix 2: *Multivariate uniform distribution of the κ values at three temperatures implies uniform distribution of the Arrhenius parameters*

Multivariate uniform distribution of the κ values at three temperatures means that the probability density $\rho_\kappa(\boldsymbol{\kappa})=\rho_\kappa(\kappa(T_1),\ \kappa(T_2),\ \kappa(T_3))$ is constant within their corresponding uncertainty ranges. It is shown here that the Arrhenius parameters $\mathbf{p}$ obtained by solving equation (1) also have an uniform distribution within their uncertainty domain in the space of $\mathbf{p}$, that is $\rho_p(\mathbf{p})=\rho_p(\alpha,n,\varepsilon)$ probability density is constant.

The transformation between variables $\mathbf{p}$ and $\boldsymbol{\kappa}$ is $\boldsymbol{\kappa}=\mathbf{T}\mathbf{p}$ (see equation (A3) in Appendix 1), which is a linear, since matrices $\mathbf{T}$ and $\mathbf{T}^{-1}$ are constant. The transformation of probability densities between the two spaces is carried out by multiplying with determinant det$\mathbf{T}$.

$$\overbrace{\rho_\kappa(\boldsymbol{\kappa})}^{\text{constant}}\ \mathrm{d}^3\boldsymbol{\kappa} = \rho_\kappa \cdot \det\left(\frac{\partial\boldsymbol{\kappa}}{\partial\mathbf{p}}\right)\ \mathrm{d}^3\mathbf{p} = \underbrace{\rho_\kappa \cdot \overbrace{\det\mathbf{T}}^{\text{constant}}}_{\rho_p(\mathbf{p})}\ \mathrm{d}^3\mathbf{p} = \overbrace{\rho_p(\mathbf{p})}^{\Rightarrow\text{constant}}\mathrm{d}^3\mathbf{p} = \rho_p\mathrm{d}^3\mathbf{p} \qquad \text{(A6)}$$

Since $\rho_\kappa(\boldsymbol{\kappa})$ is constant, therefore $\rho_p(\mathbf{p})$ is also constant. In other words, transformation (A6) changes the volume element evenly and leaves the probability density constant, thus it will transform uniform distribution in $\boldsymbol{\kappa}$ into uniform distribution in $\mathbf{p}$.

Appendix 3: *Transformation of a constrained parameter estimation problem to an equivalent unconstrained parameter estimation task*

Code JPDAP allows fitting of equations (6) and (7) and its simplified versions for 2 Arrhenius parameters to the uncertainty values *f*. However, the following constraints also have to be considered: $0 \le \sigma_\alpha,\ \sigma_n,\ \sigma_\varepsilon$, $-1 \le r_{\alpha n},\ r_{\alpha\varepsilon},\ r_{n\varepsilon} \le 1$ and $0 \le 1 - r_{\alpha n}^2 - r_{\alpha\varepsilon}^2 - r_{n\varepsilon}^2 + 2 r_{\alpha n}\, r_{\alpha\varepsilon}\, r_{n\varepsilon}$. These constraints are taken into account in an indirect way by reformulating the original problem to an equivalent, numerically more stable unconstrained parameter estimation task. The method is presented for the 3-parameter case only; the two-parameter cases are similar.

The original parameters were the standard deviations and correlations of the Arrhenius parameters, subjected to constraints originated from the positive semi-definiteness and symmetric properties of the covariance matrix ($\boldsymbol{\Sigma}_\mathbf{p}$). This matrix has the following eigenvalue–eigenvector decomposition:

$$\boldsymbol{\Sigma}_\mathbf{p} = \mathbf{O}\boldsymbol{\Lambda}\mathbf{O}^\mathrm{T} \tag{A7}$$

Here $\boldsymbol{\Lambda}$ is the diagonal matrix of non-negative eigenvalues ($\lambda_i \ge 0$), and $\mathbf{O}$ is an orthogonal matrix ($\mathbf{O}^\mathrm{T}=\mathbf{O}^{-1}$) of the orthonormal eigenvectors $\mathbf{o}_i$. Thus the overall effect of the covariance matrix on a vector $\boldsymbol{\Theta}=(1,\ \ln\{T\},\ -\{T\}^{-1})^\mathrm{T}$, can be considered as decomposition of the vector into components parallel with $\mathbf{o}_i$, multiplying each component with λ_i, and finally adding them up. This transformation can also be seen as rotating vector $\boldsymbol{\Theta}$ from the eigenvector frame (defined by $\pm\mathbf{o}_i$'s) to Cartesian frame of $\mathbf{e}_i$'s ($\mathbf{O}^\mathrm{T}=\mathbf{e}_1\mathbf{o}_1{}^\mathrm{T}+\mathbf{e}_2\mathbf{o}_2{}^\mathrm{T}+\mathbf{e}_3\mathbf{o}_3{}^\mathrm{T}$), multiplying the Cartesian coordinates with non-negative λ_i ($\boldsymbol{\Lambda}=\lambda_1\mathbf{e}_1\mathbf{e}_1{}^\mathrm{T}+\lambda_2\mathbf{e}_2\mathbf{e}_2{}^\mathrm{T}+\lambda_3\mathbf{e}_3\mathbf{e}_3{}^\mathrm{T}$), and finally rotating the vector back to Cartesian frame ($\mathbf{O}=\mathbf{o}_1\mathbf{e}_1{}^\mathrm{T}+\mathbf{o}_2\mathbf{e}_2{}^\mathrm{T}+\mathbf{o}_3\mathbf{e}_3{}^\mathrm{T}$). Here we assume that $\mathbf{e}_1(\mathbf{e}_2\times\mathbf{e}_3)=\mathbf{o}_1(\mathbf{o}_2\times\mathbf{o}_3)$, that is the two set of basis vectors are of the same handed.

The rotation angles (φ_i, where $i=1,\ldots,\ N\cdot(N-1)/2$ for N Arrhenius parameters), and the square root of the non-negative eigenvalues ($\lambda_i=\omega_i^2$, where $i=1,\ldots,\ N$) provide an unconstrained set of

parameters. This re-parameterization of equation (7) provides an expression for the standard deviation of the rate coefficient, which makes the determination of the covariance matrix straightforward as the new parameters can be varied freely, *i.e.* without constraints.

$$\sigma_{\kappa}\left(T;\varphi_i,\omega_i\right)=\sqrt{\mathbf{\Theta}^{\mathrm{T}}\cdot\mathbf{O}^{\mathrm{T}}(\varphi_1,\varphi_2,\varphi_3)\cdot\mathrm{diag}(\omega_1^2,\omega_2^2,\omega_3^2)\cdot\mathbf{O}(\varphi_1,\varphi_2,\varphi_3)\cdot\mathbf{\Theta}} \tag{A8}$$

#	reaction	α^0	n^0	ε^0 (K)	T range: uncertainty	reference	assumed Δn
1	$H_2O_2+H\rightarrow H_2O+OH$	30.813	–	1998	300–2500K: 0.4	R14 in Section 7	–
2	$H+CH_3\rightarrow H_2+{}^1CH_2$	37.076	–0.56	1350	300–1000K: 0.15 1000–1700K: 0.30 1700–2500K: 0.20	[8]	2

Table 1. Data for the reactions used as examples. Parameter α^0 is calculated with parameter A given in units mol, cm and s.

#	reaction	α^0	n^0	ε^0 (K)	ρ_p(p)	σ_α	σ_n	σ_ε(K)	$r_{\alpha n}$	$r_{\alpha\varepsilon}$	$r_{n\varepsilon}$	T range (K)	f range
R1	$H + O_2 \rightarrow O + OH$	32.964	–0.097	7560	N	5.272943	0.656768	800.271137	–0.999825	0.994015	–0.995883	800–2700	0.208–0.321
R2LPL	$H + O_2 + M \rightarrow HO_2 + M$	44.724	–1.3	0	N	1.438236	0.223583	–	–0.995378	–	–	300–2000	0.180–0.397
R3	$O + H_2 \rightarrow H + OH$	10.832	2.67	3165	N	2.163163	0.270921	195.359196	–0.998598	0.996922	–0.999675	300 – 2500	0.152 – 0.210
R4	$OH + H_2 \rightarrow H_2O + H$	19.195	1.52	1740	N	2.143215	0.286297	171.362012	–0.996541	0.991819	–0.977786	300-2500	0.103-0.308
R5	$H_2O_2 + H \rightarrow H_2 + HO_2$	23.791	1.00	3019	U	0.460517	–	–	–	–	–	300–2500	0.6
R6	$H + HO_2 \rightarrow OH + OH$	31.891	0	148	N	0.405607	–	97.899418	–	0.996676	–	500–2000	0.275–0.465
R7	$H + HO_2 \rightarrow H_2 + O_2$	15.113	2.09	–730	N	5.872579	0.706624	612.533182	–0.999948	0.993870	–0.994472	500–2000	0.277–0.529
R8	$HO_2 + OH \rightarrow H_2O + O_2$	30.834	0	–250	N	2.663322	0.320701	230.310542	–0.989621	0.965621	–0.918243	500–2500	0.387–0.468
R9HPL	$OH + OH \rightarrow H_2O_2$ (HPL)	32.236	–0.37	0	N	9.709683	1.263507	868.633251	–0.997625	0.899442	–0.867206	500–2000	0.408–0.703
R9LPL	$OH+OH+M \rightarrow H_2O_2$ +M(LPL)	40.243	–0.84	–1792	N	5.844051	0.793676	537.397524	–0.996826	0.884678	–0.853167	500–2000	0.346–0.736
R10LPL	$H + OH + M \rightarrow H_2O + M$	58.938	–2.97	399	N	2.318687	0.341781	97.736146	–0.985119	0.483772	–0.326152	300–2500	0.299–0.706
R11	$OH + OH \rightarrow H_2O + O$	10.419	2.42	–970	N	2.588877	0.347312	197.878874	–0.997980	0.999998	–0.998115	300–2500	0.177–0.347
R12LPL	$H + H + M \rightarrow H_2 + M$	39.164	–0.60	0	N	1.154390	0.219719	136.508852	–0.981868	–0.995224	0.958677	300–2500	0.376–0.759
R13	$HO_2 + HO_2 \rightarrow H_2O_2 + O_2$	25.606	0	–820								300–800	
		33.676	0	6030	U	0.307011	–	–	–	–	–	800–2500	0.4
R14	$H_2O_2 + H \rightarrow H_2O + OH$	30.813	0	1998	U	0.307011	–	–	–	–	–	300–2500	0.4
R15	$CO + OH \rightarrow CO2 + H$	12.315	1.90	–584	N	1.423152	0.207394	49.379834	–0.996044	–0.956388	0.926649	700–2500	0.189–0.310
R16	$HCO + M \rightarrow H + CO + M$	26.887	0.66	7483	N	4.517351	0.618292	292.154742	–0.999163	0.972233	–0.980992	300–2500	0.320–0.632
R17	$CO + O_2 \rightarrow CO_2 + O$	28.559	0	24005	U	0.537270	–	–	–	–	–	300–2500	0.7
R18LPL	$H + O + M \rightarrow OH + M$	42.996	–1.00	0	U	0.383764	–	–	–	–	–	300–2500	0.5
R19	$H_2O_2 + OH \rightarrow HO_2 + H_2O$	28.185	0	160								300–800	
		31.960	0	3658	U	0.230259	–	–	–	–	–	800–2500	0.3
R20	$HCO + O_2 \rightarrow HO_2 + CO$	29.657	0	206	U	0.230259	–	–	–	–	–	300–2500	0.3
R21	$HCO + H \rightarrow H_2 + CO$	32.134	0	0	N	0.383764	–	–	–	–	–	300–2500	0.5
R22	$CO + HO2 \rightarrow CO2 + OH$	11.964	2.18	9028	U	0.537270	–	–	–	–	–	500–2500	0.7

Table 2 The mean Arrhenius parameters, the assumed probability distribution $\rho_p(\mathbf{p})$ (Normal or Uniform), the parameters of the covariance matrix, the temperature range of validity and the range of uncertainty parameter f_{prior} for each investigated elementary reaction.

#	reaction	mean values							range of uncertainty						
		***m*(H₂O)**	***m*(H₂)**	***m*(Ar)**	***m*(He)**	***m*(O₂)**	***m*(CO)**	***m*(CO₂)**	***m*(H₂O)**	***m*(H₂)**	***m*(Ar)**	***m*(He)**	***m*(O₂)**	***m*(CO)**	***m*(CO₂)**
R2	$H + O_2 + M \rightarrow HO_2 + M$	10	–	0.5	0.6	–	–	–	4–16	0.05–2.55	0.2–1.0	0.2–1.0	0.2–2.0	1.0–3.0	2.0–6.0
R9LPL	$OH + OH + M \rightarrow H_2O_2 + M(LPL)$	8.33	–	1.49	–	–	–	–	2.0–15.0	1.0–4.0	0.2–1.0	0.2–1.0	0.4–1.5	1.0–3.0	0.5–2.0
R10	$H + OH + M \rightarrow H_2O + M$	6.45	–	0.38	–	–	–	–	3–15	0.5–3.0	0.2–1.0	0.2–1.0	0.2–1.0	0.5–2.5	1.2–4.5
R12	$H + H + M \rightarrow H_2 + M$	12	2.5	0.87	–	–	–	–	8–16	0.8–4.2	0.5–2.0	0.5–2.0	0.5–1.5	1.0–3.0	2.0–4.5
R16	$HCO + M \rightarrow H + CO + M$	–	2	1	1	–	1.75	–	4.0–18.0	1.5–3.0	0.5–1.5	0.5–1.5	0.5–1.5	1.0–3.0	1.5–4.5
R18	$H + O + M \rightarrow OH + M$	12	2.5	0.75	0.75	–	–	–	4.0–20.0	2.0–3.0	0.5–1.0	0.5–1.0	0.5–1.5	1.0–3.0	1.7–4.9

Table 3 Summary of the mean values and range of uncertainty of the 3rd body collision efficiencies